Gondwana Research, V. 6, No. 1, pp. 29-63.

ISSN: 1342-937X

GR Gondwana Research

Multiple Tectonothermal Events in the Granulite Blocks of Southern India Revealed from EPMA Dating: Implications on the History of Supercontinents

M. Santosh[1], K. Yokoyama[2], S. Biju-Sekhar[3] and J.J.W. Rogers[4]

[1] *Department of Natural Environmental Science, Faculty of Science, Kochi University, Akebono-cho 2-5-1, Kochi 780-8520, Japan, E-mail: santosh@cc.kochi-u.ac.jp*

[2] *Department of Geology, National Science Museum, 3-23-1, Hyakunin-cho, Shinjuku-ku, Tokyo 169-0073, Japan*

[3] *Department of Geosciences, Faculty of Science, Osaka City University, Osaka 558-8585, Japan*

[4] *Department of Geological Sciences, University of North Carolina, Chapel Hill, North Carolina 27599-3315, USA*

(Manuscript received July 12, 2002; accepted October 4, 2002)

Abstract

We report age data on zircon, monazite, uraninite and huttonite from a suite of 29 samples covering four major granulite blocks in southern India using an electron microprobe technique. The rocks analysed in this study cover all of the major lithounits in these terrains and include garnet-bearing and garnet-free charnockites, garnet-biotite gneisses, khondalites, calc-silicate rocks, and a suite of orthogneisses (biotite gneiss, biotite-hornblende gneiss). Two pink metagranites representing the magmatic phase were also analysed. Zircons from the Madras Block yield well-defined isochrons at 2.5–2.6 Ga. Core to rim analyses of single zircon grains show age zoning with 2.6–2.9 Ga igneous cores mantled by 2.4–2.5 Ga rims. Detrital zircons show age up to ca. 3.2 Ga. Monazites in this block have cores and rims with 2.5–2.3 Ga. A suite of 19 samples from the Madurai Block brings out the multiple tectonothermal events in this terrain. Zircons from an orthogneiss yield well-defined isochrons at 1.7±0.1 Ga, 0.82±0.05 Ga and 0.58±0.04 Ga from core, inner rim and rim portions, respectively. Zircon grains in other rocks preserve either core or secondary growth ages at 0.8–1.0 Ga. Zircons in a pink metagranite from this block show sharply defined isochrons of 0.68±0.03 Ga for the core and 0.57±0.01 Ga for the secondary portion. A late Pan-African overprint is observed throughout this block with zircon rims, monazite, uraninite and huttonite yielding age values in the range of 0.45–0.60 Ga. Zircons from both the Trivandrum and Nagercoil blocks show a major tectonothermal event at 0.55 Ga with faint indications of previous tectonothermal events during 0.8–1.0 and 1.7–2.0 Ga. Monazite data from both the Trivandrum and Nagercoil blocks are essentially similar to those from the Madurai Block except for presence of relic monazite in the former.

Our study confirms the notion that the Palghat-Cauvery Shear Zone marks the major terrain boundary between an Archean craton in the north and Proterozoic terrains in the south. It also strengthens the view of Paleoproterozoic accretion and Pan-African reworking of blocks south of this shear zone. The ages of production, accretion, and reworking in the terrains of southern India yield important information for the histories of Columbia (~1.8–1.5 Ga), Rodinia (~1.1–1.0 Ga), and Gondwana (~0.6–0.5 Ga) supercontinents. The southern Indian terrains formed part of a worldwide network of orogenic belts that is centered around 1.8 Ga and outlines the configuration of Columbia. Accretion of terrains in the Madurai block to Archean rocks north of the Palghat-Cauvery Shear Zone at this time is consistent with the ages suggested to be the oldest metamorphic event in the Eastern Ghats orogen of eastern India and the Rayner belt of coastal East Antarctica. Our data confirm earlier evidence that all of southernmost India underwent resetting of isotopic systems during the final accretion of Gondwana at the time of the Pan-African orogeny (~0.5 Ga). The possibility that the Trivandrum and Nagercoil terrains accreted to the Madurai block after ~0.7 Ga suggests that this Pan-African zone may also have involved accretion and closure of ocean basins. If that happened, then this zone may be the long-sought suture between East and West Gondwana.

Key words: Electron microprobe dating, granulite blocks, tectonothermal events, southern India, supercontinent history.

Introduction

Isotope geochronology provides a powerful technique to elucidate the timing of thermal events and to establish their relationship with regional and global tectonic processes. One of the ideal minerals used for dating is zircon, which has a remarkable resistance to most crustal processes, occurs as accessory phase in a variety of crustal

rocks and has low solubility in almost all melt and fluid compositions (Hanchar and Miller, 1993). High U concentration, extremely sluggish Pb diffusion and incompatibility with common Pb, mark zircon as one of the most useful minerals for tapping age information on geologic events through multiple high-temperature episodes. Despite its robust nature, however, major geologic events leave their imprints on this mineral as overgrowth or degradation. The apparent Pb loss in zircons during high-grade metamorphism results from recrystallization and growth of new grains or new rims around older grains rather than diffusion-controlled processes (Cherniak et al., 1991). Thus, investigation of the various zircon populations in a rock helps in identifying multiple thermal events. Conventional analysis of zircon populations often lead to discordant ages resulting from multiple populations that are a mixture of varying ages. The use of the single crystal method has therefore received much attention in the recent years. Monazite, another common accessory phase in crustal rocks is also a reliable mineral in dating geological events, including the emplacement age of igneous rocks and the timing of metamorphic events. With a closure temperature of over 725±25°C (Parrish, 1990), this mineral has potential utility as a geochronologic tool for a variety of crustal processes.

Modern analytical techniques rely on ion probe or laser ablation ICP-MS for dating single crystals. One of the most powerful and widely used recent techniques for dating zircons is the sensitive high-resolution ion microprobe, commonly known as the SHRIMP. Although this method yields high precision ages, it has certain limitations, first due to the high costs of SHRIMP analyses and second from its inability to locate the ion probe beam within a single growth zone in case where the mineral exhibits complex and asymmetrical zoning patterns (Hanchar and Miller, 1993).

Dating of zircon and monazite with an Electron Probe Micro Analyzer (EPMA, also commonly known as microprobe) offers an alternate technique which is much more rapid and cost effective. It has been successfully applied to obtain precision ages of magmatic and metamorphic processes (Suzuki and Adachi, 1991, 1994; Montel et al., 1996; Braun et al., 1998; Bindu, 1998; Bindu et al., 1998; Biju-Sekhar et al., 2002). Although the precision of EPMA dating is an order of magnitude below that of ion probe technique, it has the ability to determine U, Th, and Pb concentrations in domains that are ~2 μm in size. Incidentally, this is smaller than the smallest possible spot size of a sensitive high-resolution ion microprobe (SHRIMP) and considerably smaller than the sample size required for U–Th–Pb isotope dilution thermal ionization mass spectrometric (IDTIMS) method.

In this study, we apply EPMA dating technique on zircon, monazite, uraninite and huttonite from a suite of 29 samples from four granulite blocks in southern India. The samples cover a N-S traverse from the Archean cratonic margin through the Proterozoic granulite blocks up to the southern tip of the Indian Peninsula (Fig. 1). The comprehensive age data presented here have an important bearing in evaluating the multiple tectonothermal history of this Gondwana fragment and its relevance on supercontinent history.

Geologic and Geochronologic Framework

Southern Peninsular India comprises Archean cratonic nuclei surrounded by Proterozoic mobile belts. The northern part comprises a granite-greenstone (low-grade) terrain dominated by the Dharwar Craton and the southern part is made up of several granulite blocks (Fig. 1). The low-grade terrain consists largely of tonalite-trondhjemite gneisses (termed Peninsular Gneiss), associated with Archean supracrustals, granitic gneisses and a number of syn- to post-kinematic granitic plutons. In contrast, the high-grade terrain in the south consists of a collage of granulite facies terrains represented largely by charnockites (orthopyroxene-bearing rocks of acid to intermediate compositions having greasy appearance) with slivers of supracrustals and punctured at various places by acidic to basic and ultrabasic magmatic intrusives. The high-grade terrain is dissected by a number of shear zones among which the Palghat-Cauvery Shear Zone in the north and the Achankovil Shear Zone in the south are the major ones (cf. Fig. 1). The granulite terrain immediately north of the Palghat-Cauvery Shear Zone is called the Northern Granulite Block, to the east is the Madras Granulite Block and to the west, bounded on both sides by major shears, is the Nilgiri Granulite Block. To the south of the Palghat-Cauvery Shear Zone occur three granulite blocks, the Madurai, Trivandrum and Nagercoil. The status of Nagercoil as a separate crustal block is unclear, and some workers consider this as an igneous complex forming part of the Trivandrum Block (e.g., Yoshida et al., 2000).

Several recent studies have aided in unraveling the tectonic framework of the high- grade terrains of southern India, identifying a composite mosaic which resulted by the accretion of various crustal blocks from Mid-Archean to Neoproterozoic (Radhakrishna, 1989; Harris et al., 1994, 1996; Jayananda and Peucat, 1995). In the Dharwar Craton, the crust formation occurred mainly in the Archean (3.58–2.50 Ga) with a dominant event at ca. 3.0 Ga (Meen et al., 1992). South of the Palghat-Cauvery Shear Zone, the dominant crust formation is believed to

be late Archaean to Neoproterozoic (Harris et al., 1994; Jayananda et al., 1995a; Brandon and Meen, 1995; Bartlett et al., 1998; Yoshida et al., 1996).

The Nilgiri Granulite Block is separated from the Dharwar Craton by the E-W trending right lateral Moyar Shear Zone (Drury and Holt, 1980). Medium- to coarse-grained quartzofeldspathic charnockites (mostly enderbites) together with interlayered mafic granulites. Charnockites from the Nilgiri Block have been dated at ca. 2.5–2.6 Ga (Peucat et al., 1989; Jayananda and Peucat, 1996; Raith et al., 1999). The Nd model ages for the Nilgiri granulite range from 2.65 to 2.9 Ga. Their εNd values of –2.0 to +4 at 2.5 Ga suggest very short-lived or no prior crustal history of the protoliths. The granulite facies rocks in this block are characterized by high-pressure metamorphism (ca. 8–10 kbar), entrapment of high-density synmetamorphic CO_2-rich fluids from the mantle, and exhumation along an isobaric P-T path (Srikantappa, 1996).

The granulites of the Madras Block comprise largely medium- to high-pressure charnockites and gneisses. Retrograde amphibolite facies assemblages occur close to the margin of the shear zones. The granulites of this block have been dated by various methods. An early study by Vinagradov et al. (1964) report U–Pb zircon age of 2600 Ma for the Madras charnockites. Crawford (1969) dated this charnockite using Rb–Sr whole-rock method and obtained an age of 2525±125 Ma. Charnockites occurring to the south of Madras city have been dated by Sm–Nd whole-rock by Bernard-Griffiths et al. (1987) who obtained an age of 2555±140 Ma. These data suggest that the magmatic protoliths of Madras granulites accreted during 2.6–2.55 Ga and were soon involved in granulite metamorphism close to 2.5 Ga. The older ages have also been interpreted as the timing of an early granulite facies event that was later superimposed by the 2.5 Ga regional event. Madras granulites show Nd model ages ranging

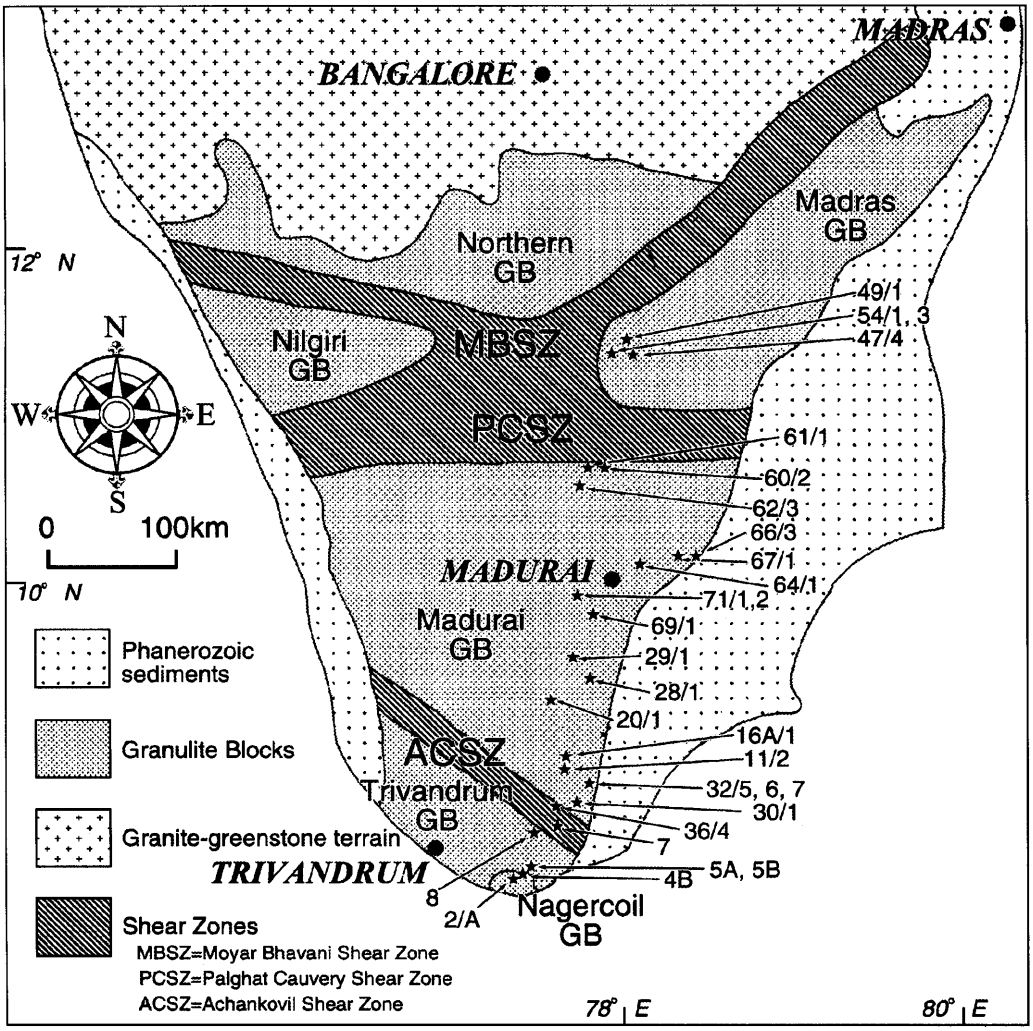

Fig. 1. Generalised geological framework of southern India showing major granulite blocks (GB) and shear zones. Locations of the samples analysed in this study are also shown.

from 2.5–2.8 Ga. They are characterized by εNd values close to zero (–0.97±1.94) at 2.5 Ga suggesting a very short or no prior crustal history of their protoliths.

The Madurai Granulite Block is located between the Palghat Cauvery Shear Zone in the north and the Achankovil Shear Zone in the south. Some of the largest highland granulite massifs in southern India (Palani, Anamalai, and Cardamom Hills) are located around the Kodaikanal region in this block. The highlands are occupied mostly by massive enderbitic charnockites while the lowlands are intercalated with metasedimentary and meta-igneous rocks. Ages of the granulite massifs range from Mid- to late Proterozoic (Jayananda et al., 1995a; Miller et al., 1996; Mohan and Jayananda, 1999). Sapphirine-bearing Mg–Al granulites in this block are characterized by ultrahigh-temperature metamorphism and multi-stage exhumation history (Raith et al., 1997; Mohan and Windley, 1993; Sajeev et al., 2001). A number of anorogenic igneous intrusives including sheets of pink granite occur in this block. U–Pb data on zircon overgrowths have yielded 1.85 Ga (Jayananda et al., 1995a), while Sm–Nd garnet-whole-rock isochron age on a charnockite sample from Kodaikkanal shows 553±15 Ma (Jayananda et al., 1995a). Bartlett et al. (1998) obtained single zircon Pb evaporation age of 2436±4 Ma from grain cores and 547±14 Ma from rims of zircons in a meta-granite sample from near Kodaikanal. The older ages have been attributed to the timing of zircon crystallization in their protoliths. The Pan-African ages obtained from the rocks of the Madurai Block (Jayananda et al., 1995a, b; Hansen et al., 1985; Bartlett et al., 1998) have been attributed to the timing of peak metamorphism in this block.

The terrain immediately south of the Achankovil Shear Zone is the Trivandrum Granulite Block, a vast supracrustal dominated terrain also known in earlier studies as the Kerala Khondalite Belt (KKB, Chacko et al., 1987). Leucocratic garnet biotite gneiss (leptynite) is the dominant lithounit, variably interlayered with aluminous supracrustals of granulite grade (khondalites) and charnockites. Quartzite, pyroxene granulite and calc-silicate rocks occur subordinately. Well constrained ages for high-grade metamorphism in this block were first provided from Sm–Nd and Rb–Sr mineral (garnet-orthopyroxene-cordierite-biotite-feldspar) and whole-rock isochrons from a cordierite and orthopyroxene-bearing charnockite at Nellikkala at the northern margin of the Trivandrum Block (Santosh et al., 1992). This study reported 539±20 Ma (Sm–Nd) and 509±41 Ma (Rb–Sr) ages that revealed the late Pan-African history of this terrain. The high-grade metamorphism was attended by copious structurally controlled influx of mantle-derived CO_2, and exhumation along a virtually isothermal decompression path (Santosh, 1987). Choudhary et al. (1992) reported Sm–Nd garnet-whole-rock ages ranging from 1793 to 558 Ma from the incipient charnockite locality at Ponmudi. Bindu (1998), Bindu et al. (1998) and Braun et al. (1998) also obtained early Proterozoic (ca. 1.9 Ga), and late Proterozoic (ca. 0.58 Ga) ages from electron microprobe dating of monazites from the Trivandrum Block. Nd isotope and zircon step-wise evaporation study by Bartlett et al. (1998) included a suite of samples from the Achankovil Shear Zone from where they obtained relatively young Nd modal ages in the range of 1.2–1.5 Ga. Combining Zr growth ages and Nd age data, Bartlett et al. (1998) inferred that the model ages resulted from mixing of detritus from Paleoproterozoic (ca. 2.0 Ga) and Neoproterozoic (1.0–0.5 Ga) age sources. Pan-African metamorphism was further confirmed by zircon ages of 533±20 Ma from the Achankovil metasediments. P-T conditions of metamorphism in the Trivandrum Block are generally in the range of 4–6 kbar and 700–880°C (Santosh et al., 1990). However, high (900°C) and ultrahigh (1000°C) temperatures have been retrieved from some localities in the northern margin, using mineral phase equilibria in charnockites (Chacko et al., 1996) and calcite-graphite thermometry in calc-silicate rocks (Satish-Kumar et al., 2002).

Pan-African activity in the Trivandrum Block continued through Cambrian to partly Ordovician when a series of pegmatites and veins were emplaced, many of which carry a variety of gemstone and rare metal mineralization (Menon et al., 1994; Semenov and Santosh, 1997). U–Pb dating of gem quality zircon from a pegmatite in the southern part of the Trivandrum Block yielded 512 Ma (Miller et al., 1996). Several K–Ar ages from gemstone pegmatites have yielded younger ages (Soman et al., 1982). Braun et al. (1998) also reported Ordovician ages (470 Ma) for monazites from the metamorphic suite in the Trivandrum Block.

The southernmost terrain at the tip of the Indian Peninsula is represented by the Nagercoil Granulite Block comprising mostly acid to intermediate charnockites of calc-alkaline affinity (Srikantappa et al., 1985; Santosh et al., 2002). This large charnockite massif is locally intercalated with exotic bands and blocks of metapelites and calc-silicate rocks plus a number of intrusives ranging from alkali syenites to norites. Mafic dykes and sills of pyroxene granulite traverse various parts of the charnockite massif. Apart from a single report of Sm–Nd and Rb–Sr isochron ages of 517±26 Ma and 484±15 Ma respectively on a garnet-bearing charnockite from the Kottaram quarry at the southern part of the massif (Unnikrishnan-Warrier et al., 1995), no detailed

geochronologic studies have yet been carried out on this block. Metamorphic P-T conditions range from 700–800°C and 5–6 kbar with low water activities effected by abundant CO_2-rich fluids within mantle isotopic signature (Santosh et al., 2002). Locally, within re-equilibrated assemblages, N_2 and CH_4 occur along with CO_2.

Sampling and Analysis

Fresh and unaltered rock samples were collected along the N-S traverse shown in figure 1, mostly from working quarries. The traverse covered, from north to south, the Madras Granulite Block, Madurai Granulite Block, Trivandrum Granulite Block and Nagercoil Granulite Block. Most of the important lithological units in each granulite block were included in the study. The sample suite for analyses thus included garnet-bearing and garnet-absent charnockites, garnet-biotite gneisses (leptynites), garnet and sillimanite-bearing metapelites (khondalites), pyroxene granulites, calc-silicate rocks, biotite gneiss, hornblende biotite gneiss and garnet hornblende gneiss. Pink granites were also included. They are foliated granitic rocks (apparently metagranites) that represent the dominant magmatic phase in this block. The sample locations, rock types and mineral assemblages as studied from thin sections are summarised in table 1.

Zircon and monazite in the analysed samples

Zircon and monazite occur as common accessories in the amphibolite and granulite facies rocks and granites analysed in this study. While zircon is a ubiquitous accessory in all the rocks, monazite is found to be more common in the pelitic gneisses and garnet-bearing charnockites. Monazite is rare or absent in the intermediate and mafic rocks, particularly in samples in which titanite and allanite occur in abundance. The lack of monazite in such cases could be attributed to increasing calcium activity resulting in titanite and allanite

Table 1. List of samples analysed together with locations, rock types and assemblages.

Sl. No.	Sample No.	Locality	Rock type	Assemblage
A. NAGERCOIL BLOCK				
1	2a	Arakkakulam	Calc-silicate	Cpx-Scp-Wo-Sph-Cc-Fo-Qz-Zr-Mz-Op
2	4b	Arakkakulam	Pyroxene granulite	Opx-Cpx-Pl-Qz-Bt-Ap-Zr-Op
B. TRIVANDRUM BLOCK				
3	5a	Kavalkkinar	Charnockite	Opx-Pl-Kfs-Qz-Bt-Ap-Zr-Op
4	5b	Kavalkkinar	Garnet biotite gneiss	Grt-Pl-Kfs-Bt-Qz-Zr-Mz-Op
5	7	Pothayadi	Garnet biotite gneiss	Grt-Pl-Kfs-Bt-Qz-Zr-Mz-Op
6	8	Krishnapudur	Khondalite	Grt-Sil-Sp-Pl-Kfs-Bt-Qz-Zr-Mz-Op
C. MADURAI BLOCK				
7	64/1	Kidaripatti	Biotite gneiss	Kfs-Pl-Qz-Bt-Zr-Op-Urt-Hut
8	61/1	Perumapatti	Calc-silicate	Cpx-Scp-Wo-Sph-Cc-Fo-Qz-Zr-Op
9	20/1	Maipparal	Charnockite	Opx-Pl-Kfs-Qz-Bt-Ap-Zr-Op
10	28/1	S.K.Patti	Charnockite	Opx-Pl-Kfs-Qz-Bt-Ap-Zr-Op
11	62/3	Kanavai	Charnockite	Opx-Pl-Kfs-Qz-Bt-Ap-Zr-Op
12	66/3	Keeravalavu	Charnockite	Opx-Pl-Kfs-Qz-Bt-Ap-Zr-Mz-Op-Urt
13	69/1	Karuvappatti	Charnockite	Opx-Pl-Kfs-Qz-Bt-Ap-Zr-Mz-Op
14	71/2	Sathankudi	Charnockite	Opx-Pl-Kfs-Qz-Bt-Ap-Zr-Mz-Op
15	71/1	Sathankudi	Garnet biotite gneiss	Grt-Pl-Kfs-Bt-Qz-Zr-Mz-Op
16	30/1	Meleppattam	Garnet biotite gneiss	Grt-Pl-Kfs-Bt-Qz-Zr-Mz-Op
17	32/5	Paraikkulam	Garnet biotite gneiss	Grt-Pl-Kfs-Bt-Qz-Zr-Mz-Op
18	32/7	Paraikkulam	Garnet biotite gneiss	Grt-Pl-Kfs-Bt-Qz-Zr-Mz-Op
19	67/1	Keeravalavu	Garnet biotite gneiss	Grt-Pl-Kfs-Bt-Qz-Zr-Mz-Op
20	32/6	Paraikkulam	Garnet charnockite	Grt-Opx-Pl-Kfs-Qz-Bt-Ap-Zr-Mz-Op
21	36/4	Ponnakudi	Garnet charnockite	Grt-Opx-Pl-Kfs-Qz-Bt-Ap-Zr-Mz-Op
22	60/2	Muttampatti	Garnet charnockite	Grt-Opx-Pl-Kfs-Qz-Bt-Ap-Zr-Mz-Op
23	11/2	Ramachandrapuram	Garnet charnockite	Grt-Opx-Pl-Kfs-Qz-Bt-Ap-Zr-Mz-Op
24	16A/1	Gangaikonda	Pink metagranite	Kfs-Pl-Qtz-Bt-Zir-Mz-Op
25	29/1	Thiruthangal	Pink metagranite	Kfs-Pl-Qtz-Hbl-Bt-Zr-Mz-Op-Urt
D. MADRAS BLOCK				
26	49/1	Minnampalli	Garnet charnockite	Grt-Opx-Pl-Kfs-Qz-Bt-Ap-Zr-Mz-Op
27	54/3	Karingalpalayam	Garnet charnockite	Grt-Opx-Pl-Kfs-Qz-Bt-Ap-Zr-Op
28	54/1	Karingalpalayam	Hornblende biotite gneiss	Hbl-Bt-Pl-Kfs-Qz-Ap-Zr-Op
29	47/4	Swamiyar Malai	Garnet hornblende gneiss	Grt-Hbl-Bt-Pl-Qz-Ap-Zr-Op

Mineral Abbreviations: Ap–apatite, Bt–biotite, Cc–calcite, Cpx–clinopyroxene, Fo–forsterite, Grt–garnet, Hbl–hornblende, Kfs–K-feldspar, Mz–monazite, Op–opaque, Opx–orthopyroxene, Pl–plagioclase, Qz–quartz, Scp–scapolite, Sil–sillimanite, Sp–spinel, Sph–sphene, Hut–huttonite, Urt–urannite, Wo–wollastonite, Zr–zircon. Sample 32/7 contains incipient charnockite patches.

constituting the major LREE phases. (Parrish, 1990). Thus, in hornblende-bearing rocks, monazite tends to be rare.

In the studied rocks, zircon occurs in a variety of forms, from euhedral grains with sharp crystal outlines to sub-rounded and rounded grains. Back-scattered electron images (BEI) of zircons show several textures in chemical composition: oscillatory igneous zoning, annealing, dissolution, secondary growth and thin bright rim (Fig. 2). Oscillatory zoning with dissolved texture is found commonly in zircons from the gneisses and granulites (Fig. 2E). Annealed core with locally irregular patches (Fig. 2F) also occur in grains from the metamorphic rocks. Zircon grains that show relatively brighter portions under BEI are usually irregular in shape and chemically homogeneous, with the bright areas developed in the core portions, along cracks or cutting the oscillatory zoning (Fig. 2C, D). In the following sections, we use the term "secondary" to describe such zircons. The grains range in size from 50 μm to 200 μm.

Monazite grains also show a wide range of shapes, from subhedral crystals with oscillatory zoning to sub-rounded and rounded grains (Fig. 3). Complex chemical

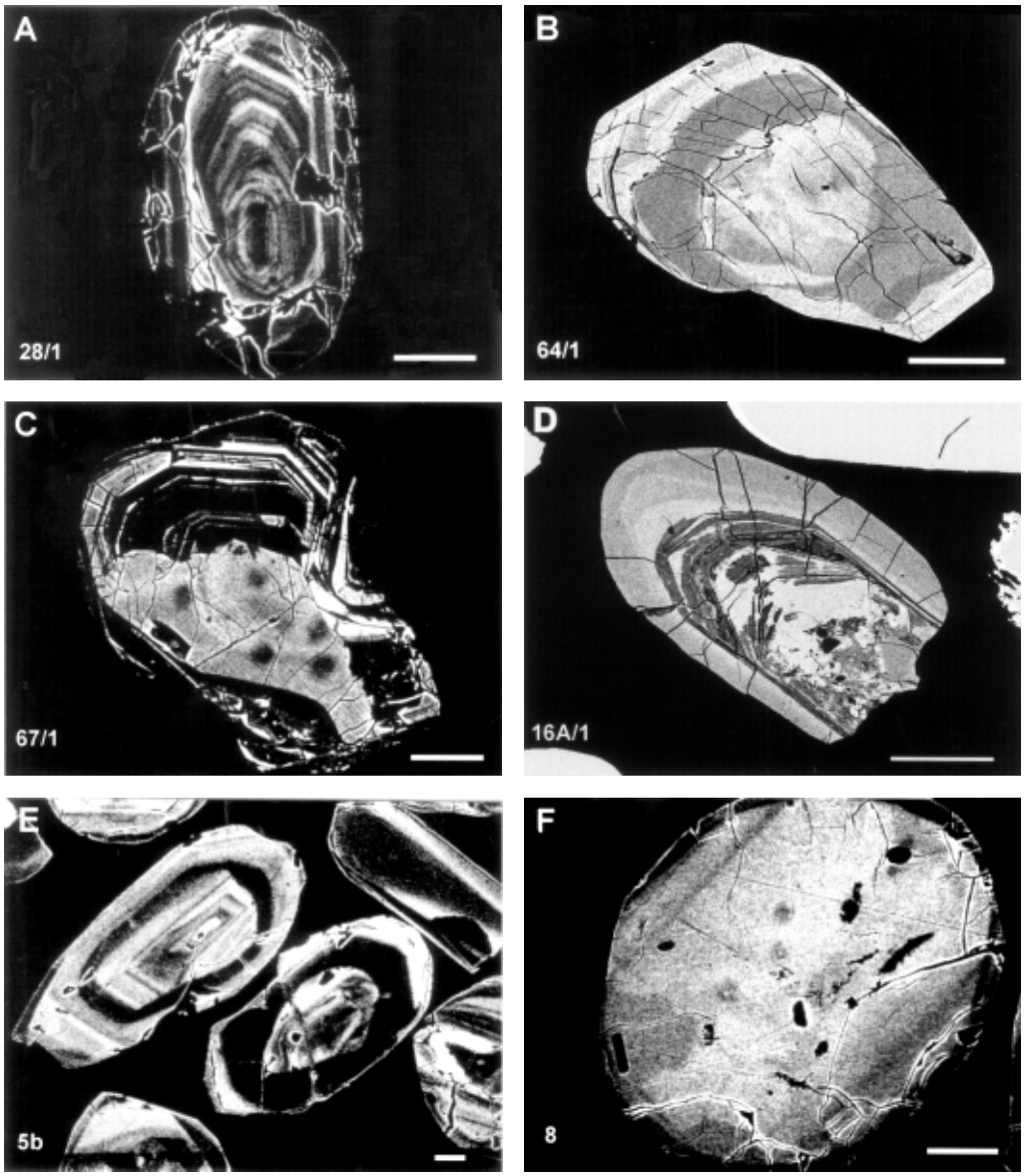

Fig. 2. Backscattered electron images of zircon grains showing various texures. A–oscillatory zoning in core, charnockite from the Madurai Block. B–complex zoning with core, inner rim and rim, biotite gneiss from the Madurai Block. C–secondary zircon recrystallized in core portion, garnet biotite gneiss from the Madurai Block. D–secondary zircon crystallized in core with oscillatory zoning, metagranite from the Madurai Block. E–dissolved core with zoned rim, garnet biotite gneiss from the Trivandrum Block. F–annealed zircon, khondalite from the Trivandrum Block. Bar scale measures 20 μm.

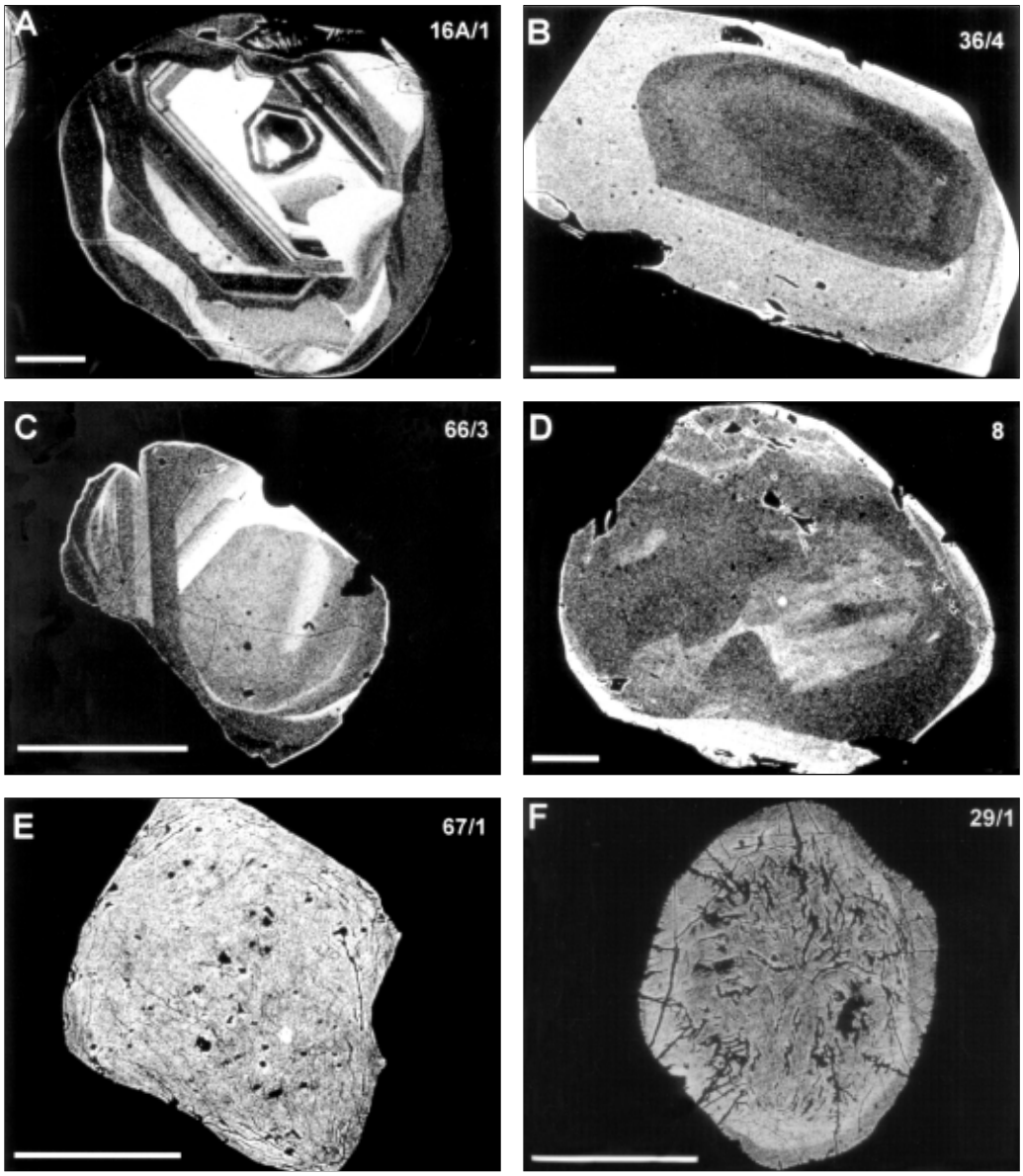

Fig. 3. Backscattered electron images of monazite and uraninite grains. A–monazite with oscillatory zoned core, pink granite from the Madurai Block. B–monazite with clear rim, garnet charnockite from the Madurai Block. C–monazite with complex zoning, charnockite from the Madurai Block. D–monazite with partly dissolved core, khondalite from the Trivandrum Block. E–uraninite grain, garnet biotite gneiss from the Madurai Block. F–uraninite with clear rim, pink metagranite from the Madurai Block. Bar scale measures 20 μm.

zoning is common in monazite grains as in the case for zircons. Overgrowths on cores are clearly marked by contrast in brightness under backscattered image. Uraninite grains occur in both metagranites and pelitic gneisses, mostly as anhedral grains, some of which display a thin and dull mantle around a bright core. Huttonite is scarce.

EPMA Chemical Dating

The theoretical basis of this study follows that of the chemical thorium uranium total Pb isochron method (CHIME) described by Suzuki et al. (1991).

First, the apparent age (t) is calculated from each set of the UO_2, ThO_2 and PbO analyses (wt.%) by solving the equation:

$$\frac{PbO}{W_{Pb}} = \frac{ThO_2}{W_{Th}} \left\{\exp(\lambda_{232}t) - 1\right\} + \frac{UO_2}{W_U}\left[\frac{\exp(\lambda_{235}t) + 138\exp(\lambda_{238}t)}{139} - 1\right] \quad (1)$$

Where W symbolizes the gram-molecular weight of each oxide (W_{Pb} = 224, W_{Th} = 264 and W_U = 270) and λ symbolizes the decay constant of each isotope

(λ_{232} = 4.9475 × 10^{-11}/yr, λ_{235} = 9.8485 × 10^{-10}/yr and λ_{238} = 1.55125 × 10^{-10}/yr; Steiger and Jäger, 1977). To eliminate the effect of variations in the Th/U ratio on total Pb produced over a given time span, we turn the sum of ThO_2 and UO_2 into ThO_2* by:

$$ThO_2^* = ThO_2 + \frac{UO_2 W_{Th}}{W_U \{\exp(\lambda_{232} t) - 1\}} \times \left[\frac{\exp(\lambda_{235} t) + 138 \exp(\lambda_{238} t)}{139} - 1 \right] \quad (2)$$

The best-fit regression line is determined by the procedure of York (1966), taking into account the uncertainties in microprobe analysis, and calculating the first approximation of age (T) from the slope (m) of the following equation:

$$T = \frac{1}{\lambda_{232}} \ln \left[1 + m \times \frac{W_{Th}}{W_{Pb}} \right] \quad (3)$$

$$\text{and } m = \frac{PbO}{ThO_2^*} \quad (4)$$

Following this, the second approximation is to replace the apparent ages (t) of Eq. (2) with the first approximation (T) and calculate the ThO_2^{*2}, and get T2 by equation (3), using the ThO_2^{*2} in place of ThO_2-. The same procedure is repeated for n times until the difference between T_n and T_{n-1} becomes negligible. Suzuki and Adachi (1991) obtained both initial PbO content and age from the regression line on the PbO–ThO_2* diagram, assuming that initial PbO is homogenously present in the mineral. Recent studies have shown that the initial Pb is negligible in comparison with radiogenic Pb (Montel et al., 1996). Hence in this study, the ages have been calculated assuming that initial Pb is zero. This method is essentially the same as the early theoretical method of absolute age estimation from the wet chemical analyses by Holmes (1931).

Sample preparation and analysis

Fresh rock pieces were crushed into fine fractions using a stainless-steel stamp mill. The powdered samples (<100 mesh size) were first cleaned using water to remove the dust particles, and then dried in an oven. The magnetic minerals were then removed using hand magnet. Heavy fractions were separated by methylene iodide with specific gravity around 3.3. They were mounted on glass slides using epoxy resin and subjected to diamond polishing. Both polished grain mounts and normal thin sections were used for the study of grain characteristics and EPMA analyses.

Chemical analyses were made using an electron microprobe (JEOL JXA-8800) at the National Science Museum, Tokyo, Japan. The analytical conditions are 15kV accelerating voltage, 0.5 μA probe current (0.2 μA for monazite), 2 μm probe diameter and 200–300 seconds counting time for U, Th and Pb. PRZ corrections (modified ZAF) are applied for the analyses. Standard materials for U, Th and Pb are synthesized γ-UO_3, ThO_2 and natural crocoite ($PbCrO_4$), respectively. Natural and synthesized minerals were used as standards for other elements. Seven elements (Si, Zr, Y, Hf, U, Th, Pb) for zircon and 14 elements (P, Si, La, Ce, Pr, Nd, Sm, Gd, Dy, Y, U, Th, Pb, Ca) for monazite were analyzed. UMα, ThMα, PbMα lines are used in the U, Th and Pb analyses, respectively, and the spectral interferences of the ThMζ, YLχ and ZrLγ lines with the PbMα line, and the ThMβ line with the UMα line were corrected.

Age calibrations were carefully performed by comparing data obtained from zircons and monazites by EPMA dating with those generated by SHRIMP technique. Apart from minor shifts due to machine drift and standard conditions, the ages obtained from both techniques were found to be well consistent. Internal age standards are 994±5 Ma zircon from an Antarctic rock analysed by SHRIMP and 3019±4 Ma monazite from Australia (Kiyokawa et al., 2002, unpublished data). The latter is the SHRIMP age of the coexisting zircon. Both internal standards are routinely analyzed before and after the analyses of unknown samples. Further discussion on chemical U–Th–Pb dating using electron microprobe can be found in Montel et al. (1996). As there is no suitable internal standard for uraninite and huttonite, their ages were calibrated using the same method adopted for monazite.

The error (1-sigma confidence level) of age measurements for each zircon analysis includes instrumental counting statistic only, and is approximately 3% at PbO = 0.05 wt.% to c. 10% at PbO = 0.02 wt.% level. Least-square fitting is applied to calculate the age for a linear regression line with an assumption that each data set belongs to a single thermal event. In some paragneiss samples, age of zircon core is different from grain to grain, indicating contribution from multiple sources. Age values from monazite, uraninite and huttonite have higher precision, and the estimate error in age is usually less than a few percent.

Results

From the many grains of zircon, monazite, uraninite and huttonite in the 29 samples that we analysed in this study, a comprehensive database was generated from several hundreds of analyses. Since it is beyond scope to

include all of the analytical data in this paper, we present only the representative analytical data as tables A-1 to A-10 in the Appendix, but assemble the primary data within figures accompanying the following sections. The results from individual granulite block will be briefly discussed in the following sections.

Madras Block

From the Madras Block, four representative samples were analysed for monazite and zircon which include garnet-bearing charnockites (54/3, 49/1), hornblende biotite gneiss (54/1), and garnet-hornblende gniess (47/4). Out of these, monazites were obtained only in a garnet-bearing charnockite (49/1). Representative analytical data from zircons are given in table A-1.

An example of variation in spot ages within zircon grains from this block is shown in figure 4, where backscattered images of three representative zircon grains and their sketches with corresponding ages obtained from various zones in each grain are shown. Zircons from the garnet-hornblende gneiss (Fig. 4A) and garnet-bearing

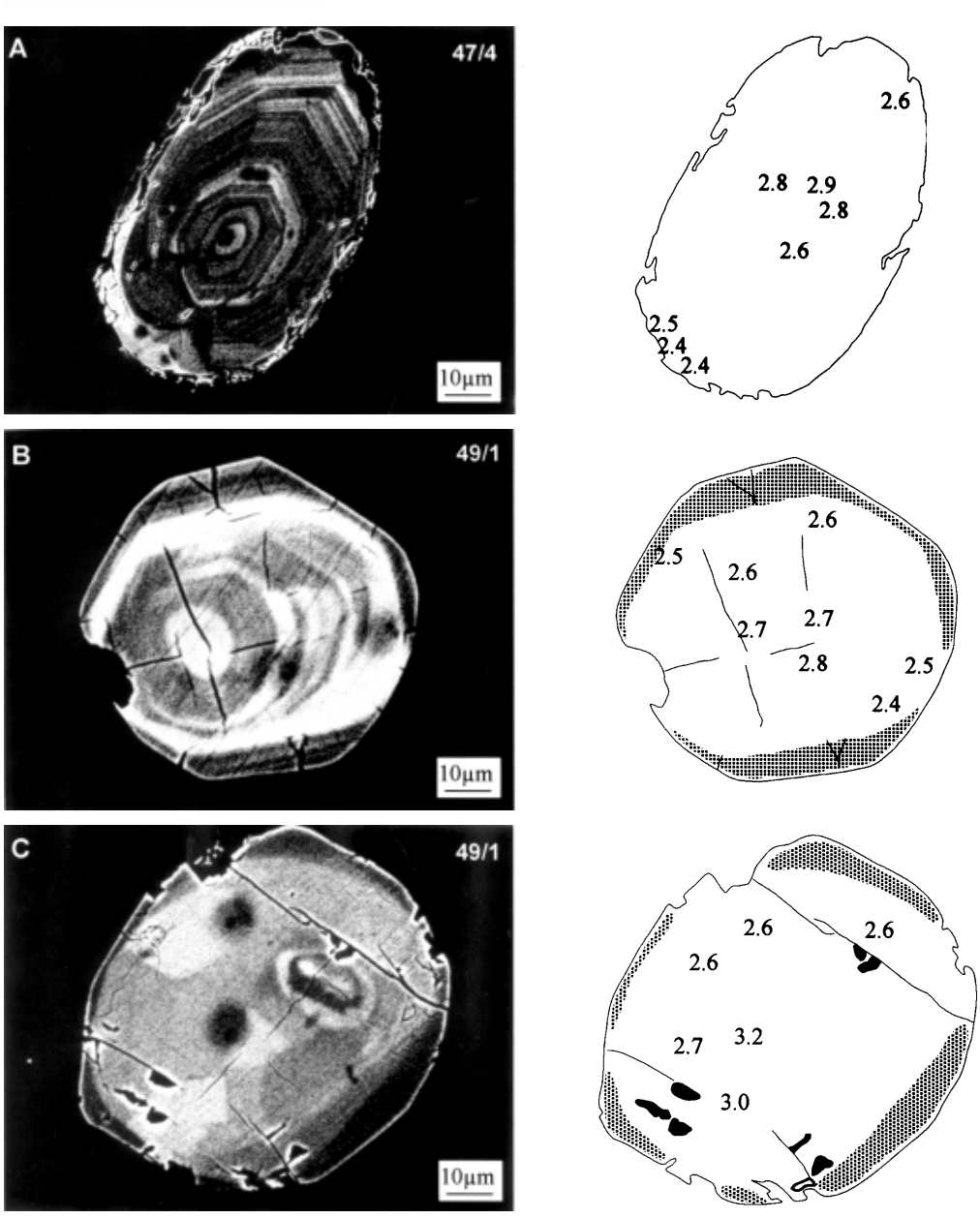

Fig. 4. Backscattered electron images of zircon grains from the Madras Block and age values from core to rim in each grain as obtained in this study. (A) Zircon from garnet hornblende gneiss (47/4). (B, C) Zircons from garnet charnockite (49/1).

charnockite (Fig. 4B, C) show distinct age variation from central to marginal portions. The core portions are characterized by older ages (up to 3.2 Ga), while the marginal portions show younger ages. Zoned grains with a thin mantle of overgrowth (Fig. 4A, B) show 2.6–2.8 Ga at the oscillatory core and 2.4–2.5 Ga at the rim. The third grain (Fig. 4C), which is rounded with no pronounced zoning patterns, shows an older inherited core (3.2 Ga).

PbO vs. ThO_2* plots for zircons from two charnockites (54/3, 49/1) and one hornblende biotite gneiss (47/4) from the Madras Block are shown in figure 5. In all cases, the plots except for secondary/inherited zircons show remarkable linear arrays, yielding sharply defined isochrons with ages in the range of 2.63±0.03 to 2.49±0.03 Ga.

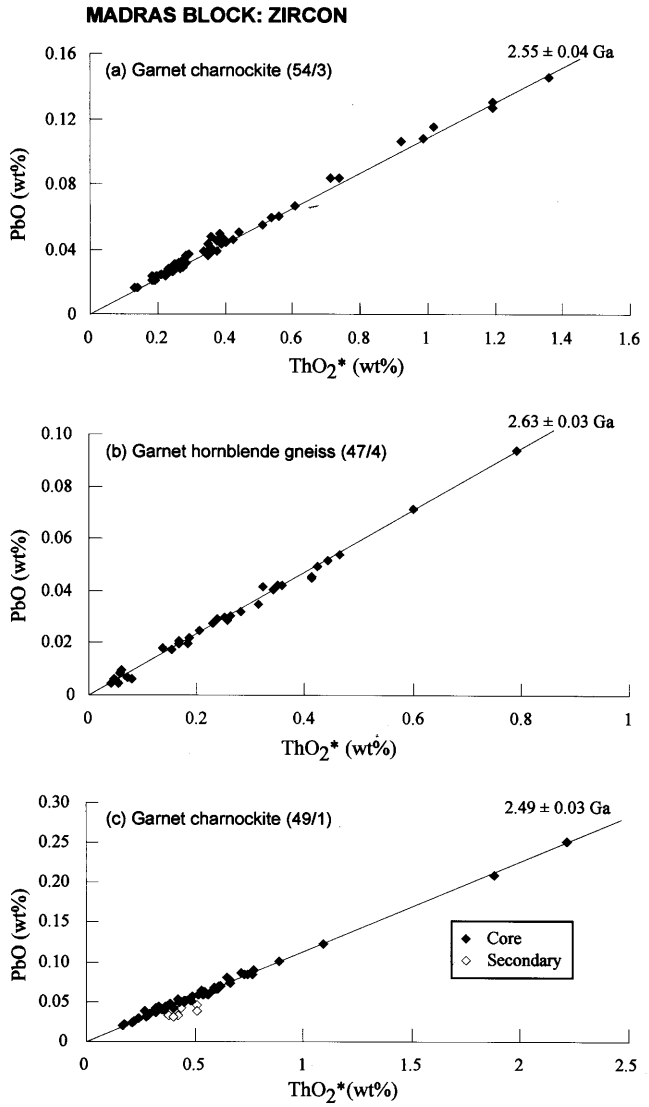

Fig. 5. ThO_2* vs. PbO plots showing isochrons of zircon data from the Madras Block. (a) Garnet charnockite (sample 54/3), (b) garnet hornblende gneiss (sample 47/4) and (c) garnet charnockite (sample 49/1).

Age data on zircon grains in various samples from the Madras Block are compiled in figure 6. Ages obtained from the grain cores mostly range between 2.4–2.7 Ga with peak at 2.6 Ga. Still older ages (2.8–3.2 Ga) present in some samples could indicate an earlier event of accretion, since such accretion event has been reported from further west of the study in the Eastern Dharwar Craton (Jayananda et al., 2000). A linear array for rims in the zircons was obtained only in one sample (54/3). Overgrowths in the zircons span a wide range of ages from 1.7 to 2.6 Ga. Importantly, all the samples from this block display common core ages in the range of 2.4–2.6 Ga.

Age data on monazites grains in the Madras Block come from a garnet-bearing charnockite (49/1). Monazite in this rock shows low U and Th contents (0.57–1.13% ThO_2 and 0.052–0.055 UO_2) with the ages in the range of 2.3–2.5 Ga.

Madurai Block

A total of 19 rock samples were analysed from the Madurai Block which include four garnet-bearing charnockites (36/4, 32/6, 11/2, 60/2), six garnet-free charnockites (20/1, 28/1, 69/1, 71/2, 66/3, 62/3), five garnet biotite gneisses (30/1, 32/5, 32/7, 71/1, 67/1), one biotite gneiss (64/1), one calc-silicate rock (61/1) and two pink metagranites (16/A1, 29/1). While zircon grains were analysed from all the samples, monazites were available in only eight of them (36/4, 30/1, 11/2, 16A/1, 66/3, 67/1, 60/2 and 61/1). We also analysed uraninite from pink metagranite (29/1), garnet biotite gneiss (67/1), biotite gneiss (64/1), and garnet-free charnockite (66/3), as well as huttonite from biotite gneiss (64/1). The representative analytical data on zircons from charnockite (both garnet-bearing and garnet-free) are given in table A-2 and those on garnet-biotite gneiss, biotite gneiss, calc-silicate and pink metagranite are given in table A-3. Representative monazite analyses from charnockites are given in table A-4 and those from garnet biotite gneiss and pink metagranite are given in table A-5. Analytical data on uraninite and huttonite are summarized in table A-6.

PbO vs. ThO_2* plots of zircon grains from biotite gneiss (64/1) are shown in figure 7. The plots display three distinct populations in the isochron diagram with well-defined age groups from cores, inner rim zones and rims of individual grains (cf. Fig. 2B). In the isochron diagrams, the core values yield an age of 1.7±0.1 Ga, the inner rims yield 0.82±0.05 Ga and the (outer) rims yield younger ages of 0.58±0.04 Ga. A multiple metamorphic imprint ranging from Paleoproterozoic through Neoproterozoic to late Proterozoic in the Madurai Block is clearly preserved in this sample.

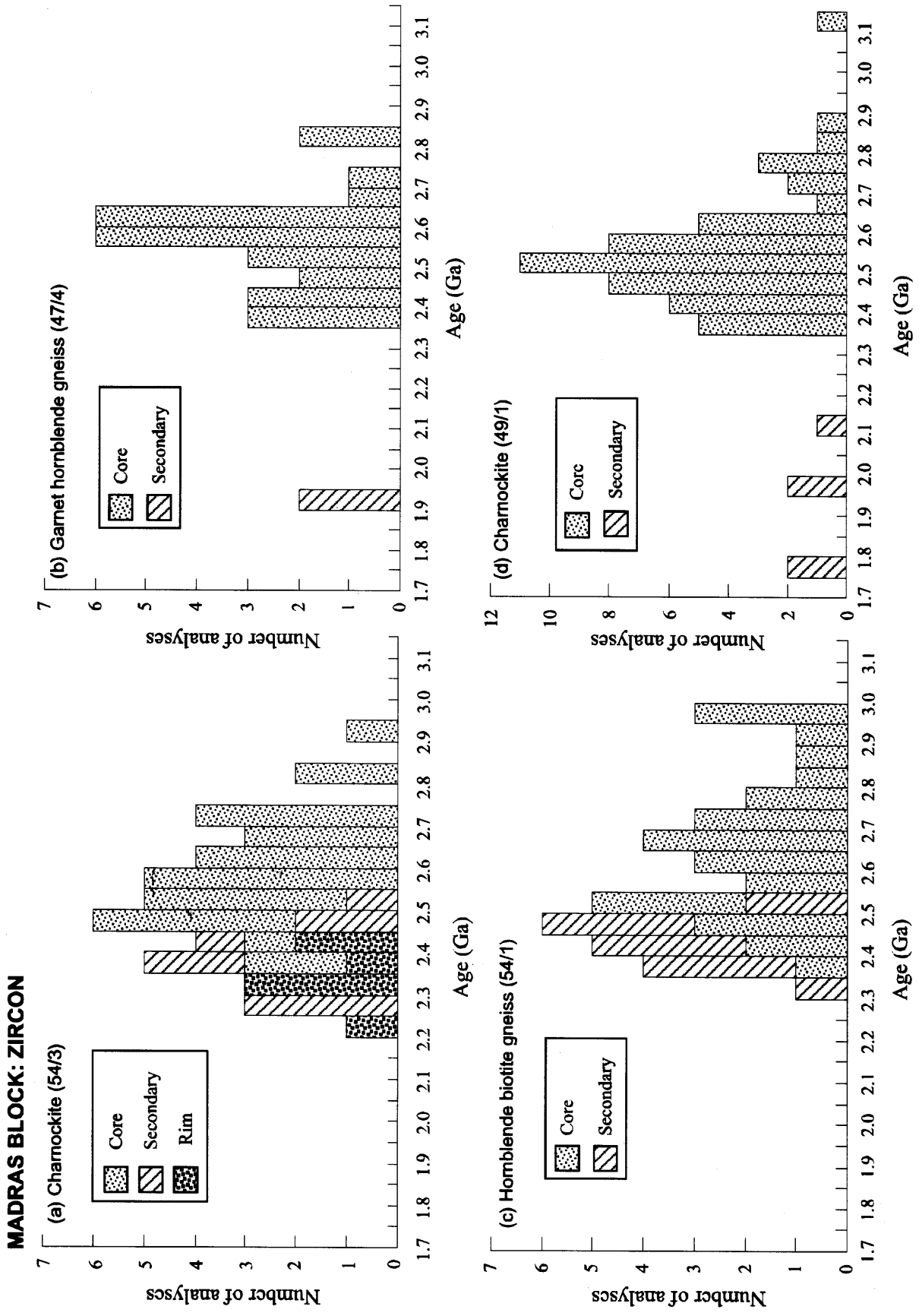

Fig. 6. Histograms showing age data from the cores, rims and secondary portion of zircons in the Madras Block samples.

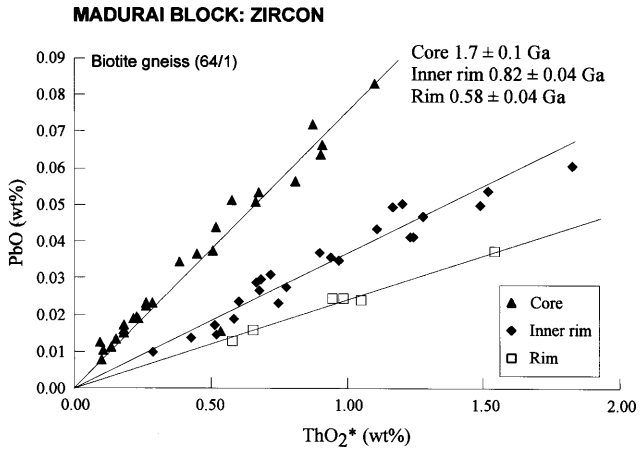

Fig. 7. ThO_2* vs. PbO plots for core, inner rim and rim of zircons from an orthogneiss (64/1) in the Madurai Block. The plots define three isochrons with distinct age values.

The above data, however, markedly contrast with the PbO vs. ThO_2* plots of zircons from the pink metagranite (16A/1) where the data define two isochrons with an age of 0.68±0.03 Ga for the core and 0.57±0.01 Ga for the rims (Fig. 8). Clearly, these zircons preserve no older record and are minerals that newly crystallized from magmas that intruded during Pan-African time. Core portions in the zircons also show clear magmatic zonation in backscattered electron images (Fig. 2D). The isochron age of the secondary (overgrowth) zircon from this granite is closely comparable with that from the rim ages of zircons in the biotite gneiss sample (64/1) discussed above.

Age data in zircons from various samples in the Madurai Block are compiled in figure 9. Data from the metamorphic rock suite show a common prominent peak at 0.8–1.0 Ga, whereas the peak age for the pink metagranite is ca. 0.7 Ga. The biotite gneiss sample (64/1) yields an additional peak at 1.7 Ga. Some sparse older ages of up to 2.3 Ga are also present in few samples, which could be correlated to the Paleoproterozoic magmatic accretion event recorded by Jayananda et al. (1995a) and Bartlett et al. (1995, 1998). An evaluation of the data from individual samples shows that the most common range of core and secondary ages are between 0.80–1.0 Ga in the metamorphic rocks, while the granite samples define a narrow range of ca. 0.70 Ga. It is evident that new zircons (cores) crystallized in the Madurai Block during at least two major events, one at ca. 1.7 Ga and the other at ca. 0.8–1.0 Ga. The rocks of the Madurai Block also carry zircons having rims or overgrowths with ages closely comparable with the cores at 0.7–0.8 Ga, without any significant age zoning. However, prominent overgrowths with ages ranging from 0.45–0.65 Ga are also present in some grains. In the biotite

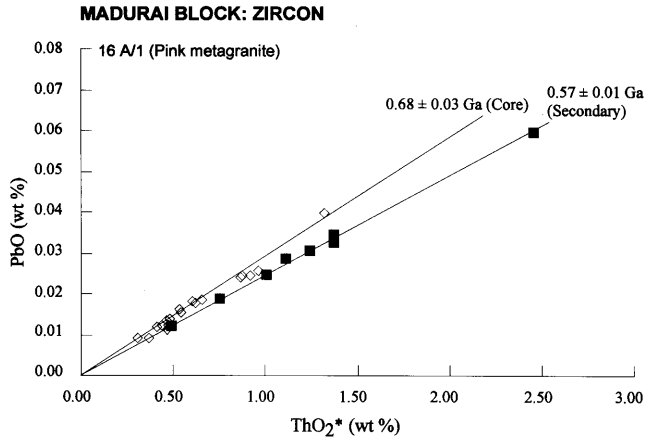

Fig. 8. ThO_2* vs. PbO plots for core and secondary of zircons in a pink metagranite (16A/1) in the Madurai Block. The plots define two distinct isochrons.

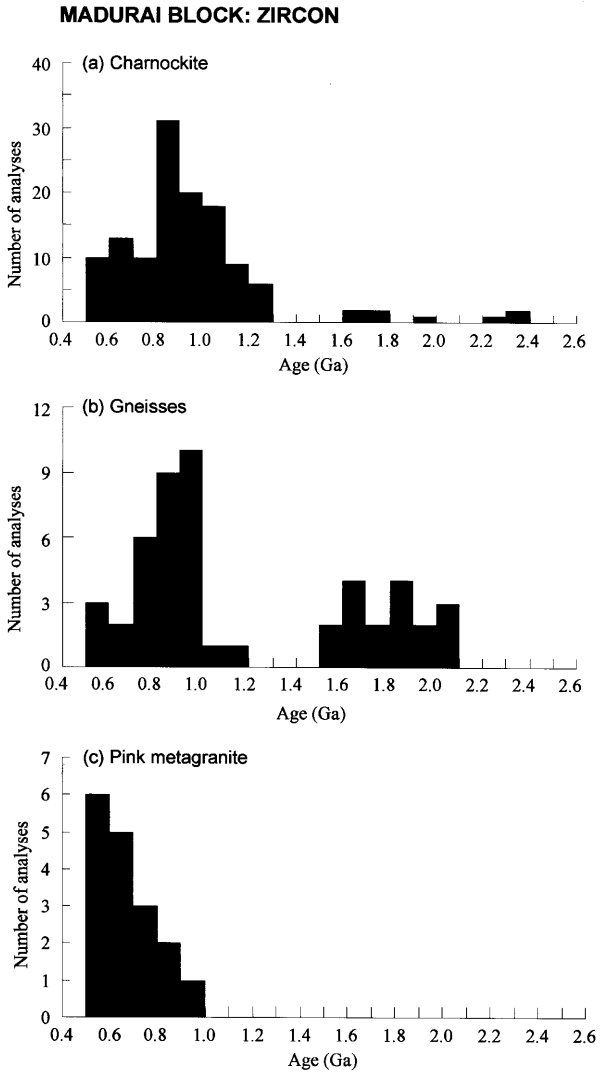

Fig. 9. Histograms showing age data from selected zircons (PbO>0.02 wt.%) in the metamorphic and magmatic suites of rocks from the Madurai Block.

gneiss, some charnockites and the pink metagranite, the rim ages define a more restricted range (0.57–0.6 Ga).

Monazite grains from the Madurai Block show complex age zoning, although clear plateau ages are often observed in some samples (Fig. 10). Age data on monazite in different samples from the Madurai Block are plotted in figure 11. Monazite in the pink metagranite (16A/1) shows tightly constrained ages of 0.51–0.57 Ga with peaks at 0.54 – 57 Ga for the core and 0.51–0.52 Ga for the rim. Monazites from garnet charnockites show 0.48–0.58 Ga,

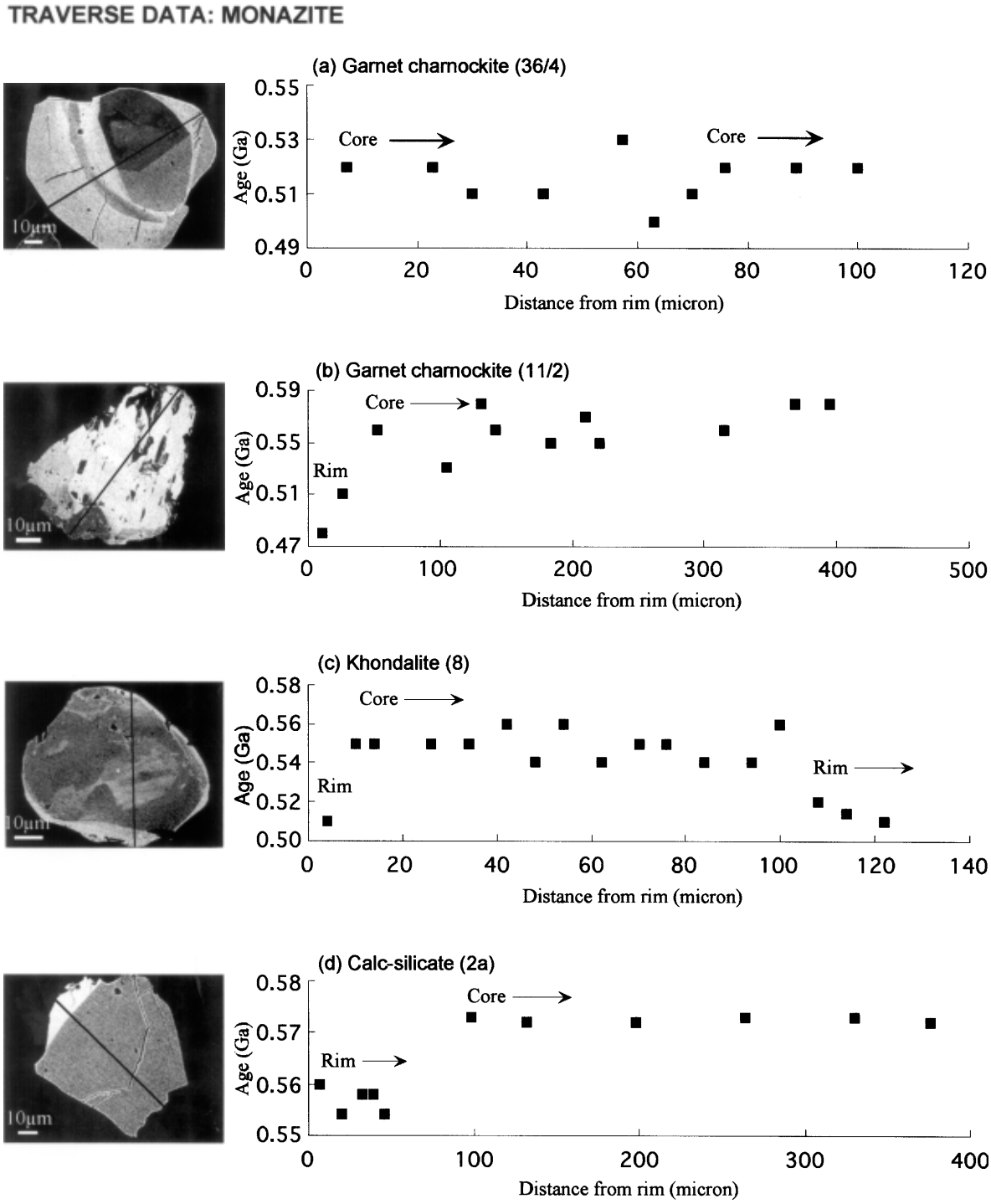

Fig. 10. Electron microprobe traverse in monazite grains from the southern granulite block. (a) Plateau with 0.50–0.53 Ga in garnet charnockite (36/4) in the Madurai Block, (b) plateau of 0.55–58 Ga and rim of 0.48 Ga in garnet charnockite (11/2) in the Madurai Block, (c) plateau of 0.54–0.56 Ga in khondalite (8) in the Trivandrum Block, (d) plateau of 0.57 Ga and rim of 0.55 Ga in the calc-silicate (2a) in the Nagercoil Block.

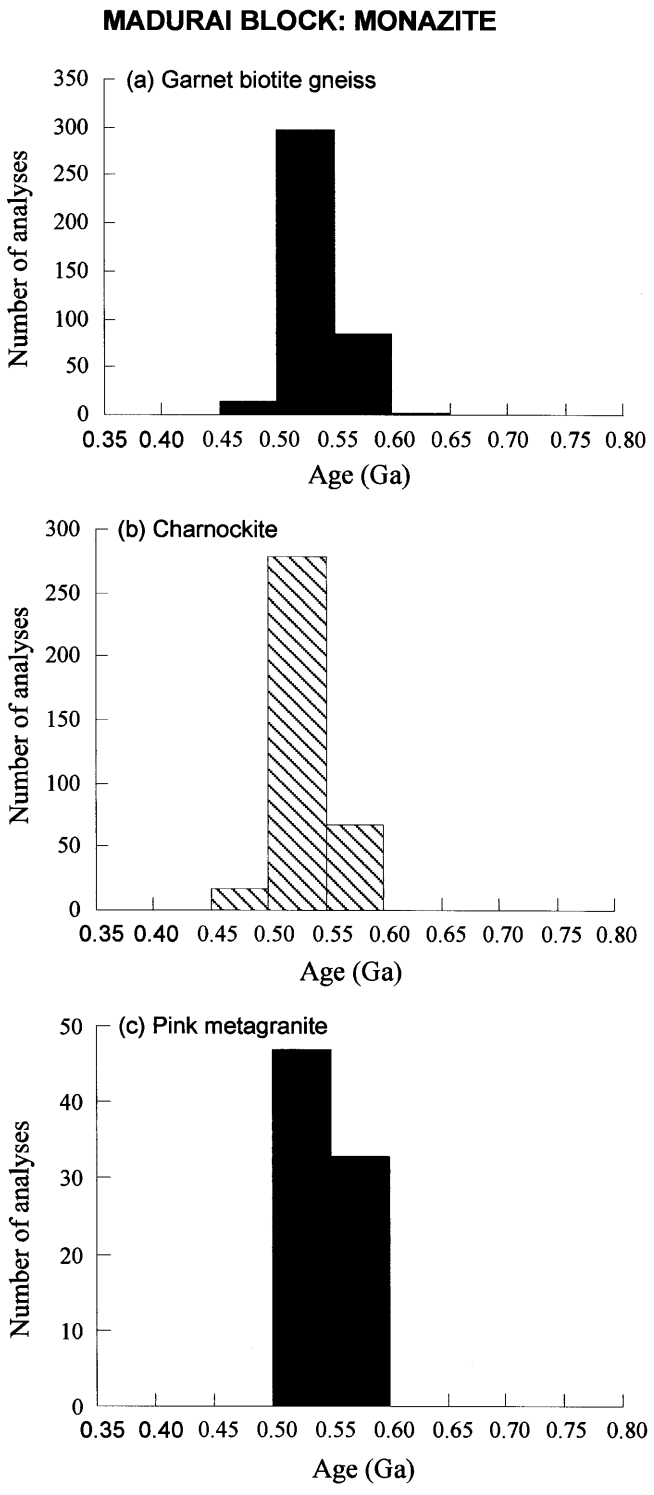

Fig. 11. Histograms assembling age data from monazite in the Madurai Block.

with peaks at 0.52–0.58 Ga for the core and 0.48–0.52 Ga for the rim. Monazite is absent in most of the garnet-free charnockites. One sample (66/3) that contained monazite yielded an age of 0.53–0.56 Ga for the core and 0.51–0.52 Ga for the rim. In the garnet-biotite gneisses, monazites yield 0.52–0.59 Ga for the core and 0.46–0.53 Ga for the rim. Although igneous activity older than 0.6 Ga is confirmed by zircons, all of the monazite in this block was less than 0.6 Ga old.

The age data from uraninite and huttonite in the Madurai Block are assembled in figure 12. Uraninite grains from the pink metagranite (64/1), charnockite (66/3), garnet biotite gneiss (67/1) and biotite gneiss (64/1) show a tightly constrained range of 0.51–0.54 Ga for the core and 0.45–0.51 Ga for the rim. Huttonite from the biotite gneiss (64/1) yields a sharply constrained age of 0.54 Ga for the core and 0.51 Ga for the rim. Although age values of uraninite and huttonite were computed without internal standards, it is important to note that their results are well consistent with those from coexisting monazites.

Trivandrum Granulite Block

Samples analysed in this study from the Trivandrum Block include one garnet-free charnockite from the southeastern margin of the block in contact with the Nagercoil Block (5A), two garnet-biotite gneisses (5B, 7) and one khondalite (8). Representative analytical data on zircons are given in table A-7 and those on monazites are given in table A-8.

Age data on zircons from the Trivandrum Block are shown in figure 13. Although the data display a wide range of core ages from ca. 0.4 Ga up to 2.8 Ga, almost all zircons rims preserve the age of ca. 0.55 Ga.

Age data on monazites from the Trivandrum Block are compiled in figure 14. The data define a total spread at 0.46–0.61 Ga. Most of the core ages lie between 0.50–0.55 Ga with one exception of up to 0.6 Ga in the khondalite (sample 8). These results are consistent with the CHIME ages from monazites reported by Bindu et al. (1998) from the northern part of this block. Rim values also define a tight range, from 0.46 to 0.52 Ga, with an exception of 0.55 Ga in the khondalite. Relic monazites with older ages are present in both the garnet biotite gneisses, but absent in khondalite. The oldest and youngest monazites are about 1.9 Ga and 0.7 respectively (Fig. 13), consistent with the reports from this block by Bindu (1998), Bindu et al. (1998), Bartlett et al. (1995, 1998) and Braun et al. (1998).

Nagercoil Granulite Block

Zircon from a pyroxene granulite (4B) and zircon and monazite from a calc-silicate rock (2A) were analysed from this block. Although zircon is present in both samples, those from the pyroxene granulite have too low UO_2 and had to be excluded. Table A-9 therefore summarises analytical data from the calc-silicate rock only.

Age data on monazites and zircons from the Nagercoil Block are shown in figure 15. Monazite from the calc-

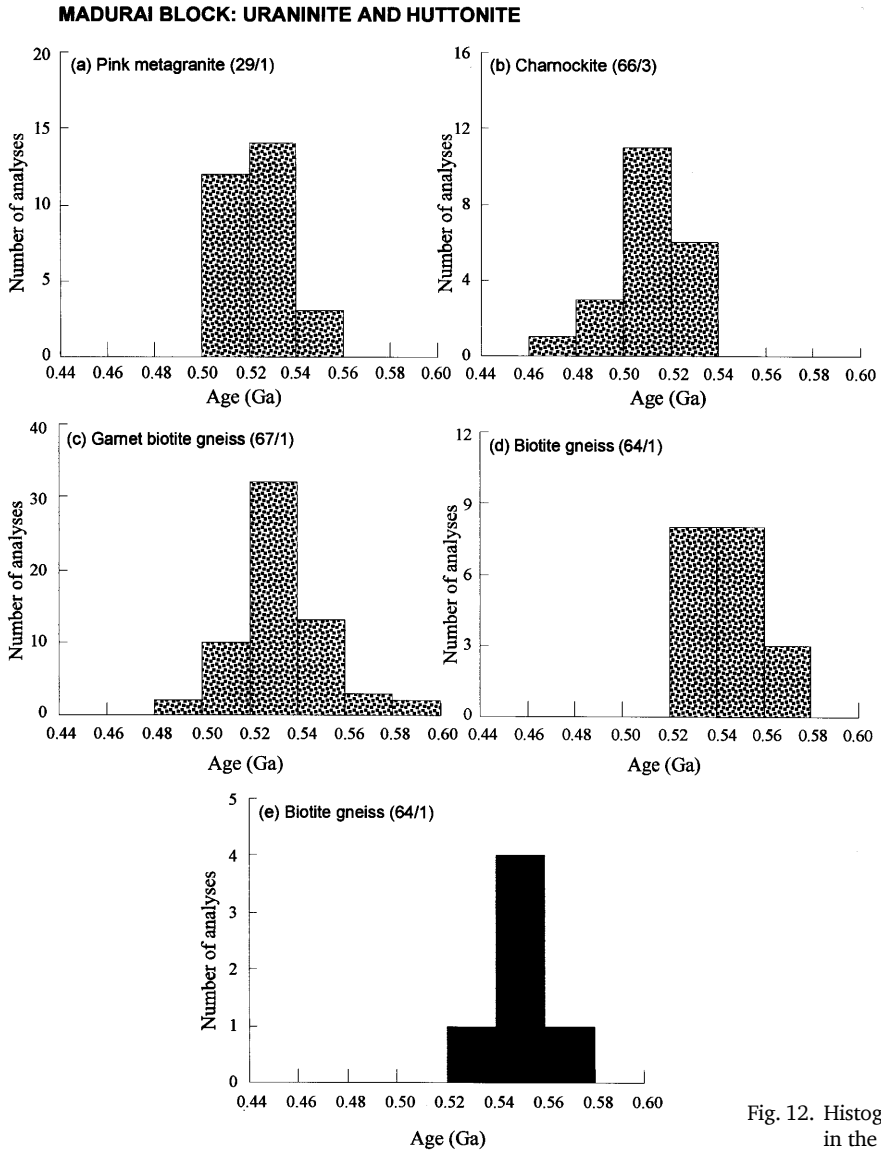

Fig. 12. Histograms showing age data from uraninite and huttonite in the Madurai Block.

silicate rock shows a narrow spread between 0.50–0.61 Ga. The core and rim ages lie between 0.55–0.61 and 0.50–0.55 Ga, respectively. While most monazite grains in this sample show results similar to those in the Madurai and Trivandrum Blocks, some grains preserve relict ages in the range of 1.8 to 1.0 Ga. No isochrons were obtained from the zircon data in this block. Both the cores and rims of zircons from the calc-silicate are variable in range: cores of zircons show 1.3 to 2.6 Ga and rims show 0.5 to 0.8 Ga ages.

Discussion

EPMA dating of zircon, monazite, uraninite and huttonite from four granulite blocks in southern India yields important information on multiple tectonothermal events in this Gondwana fragment. Despite the large spread in age data from some blocks, our study brings out sharp peaks at definite age intervals and dominant populations characterizing the major event in each block (Figs. 16, 17).

Madras Granulite Block

Age data computed from EPMA analyses of zircons from the Madras Block yielded well-defined isochrons at 2.63±0.03 Ga, 2.55±0.04 and 2.49±0.03 Ga. These ages are closely comparable with the whole-rock Sm–Nd isochron age of 2.55±140 Ma obtained by Bernard-Griffiths et al. (1987) on a charnockite from Madras. It is believed that the magmatic precursors of the Madras granulites accreted during 2.6–2.55 Ga and were subjected to granulite facies metamorphism at 2.5 Ga, with available

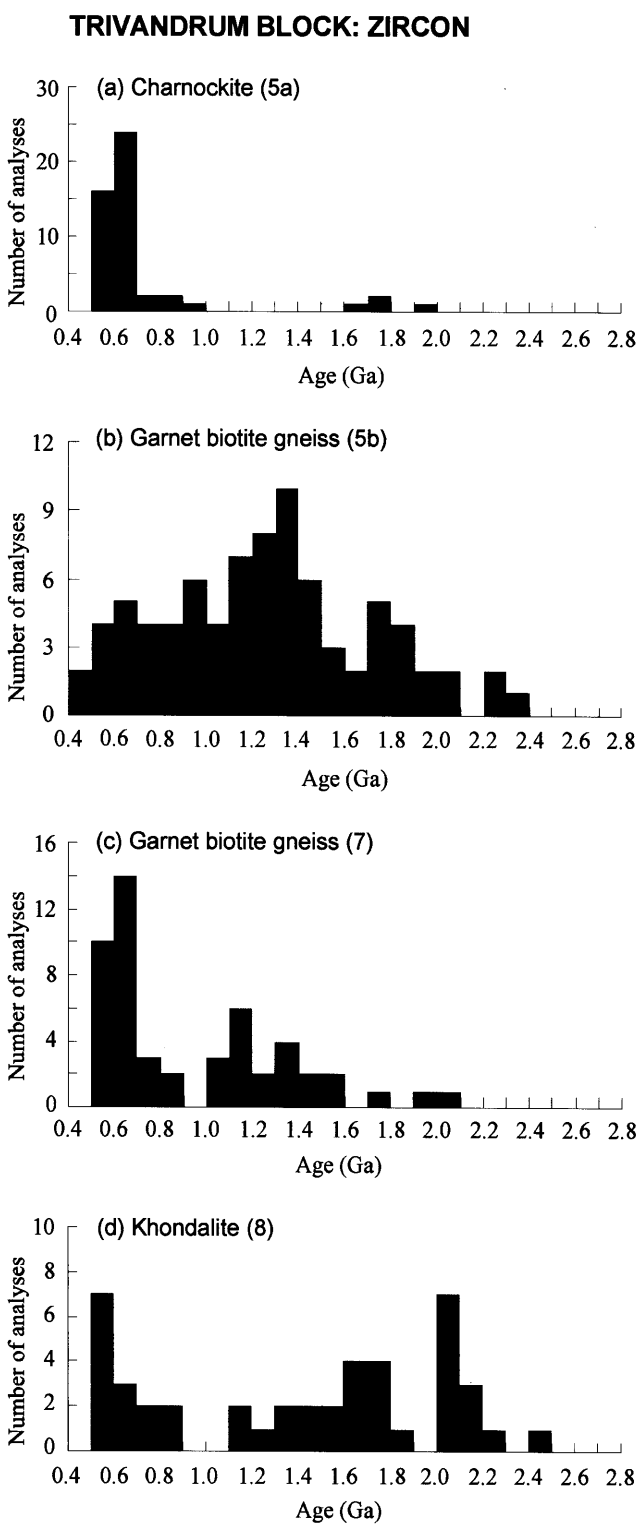

Fig. 13. Compiled histograms of age data on zircons from the Trivandrum Block.

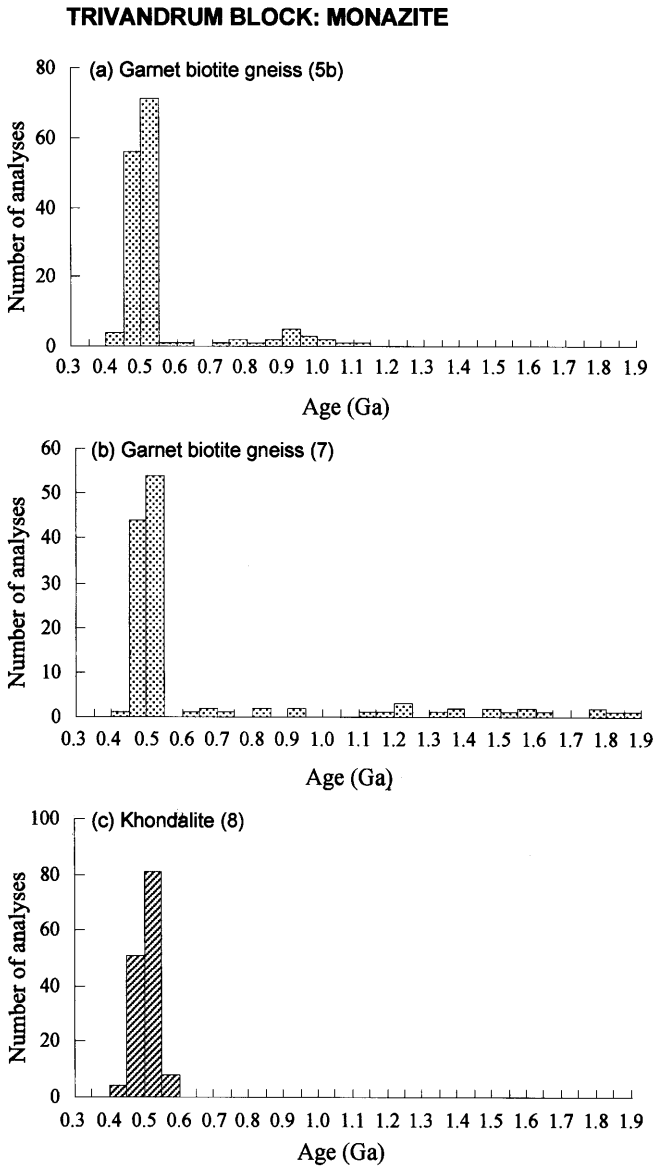

Fig. 14. Compiled histograms of age data from monazite in the Trivandrum Block.

Nd data suggesting a very short crustal residence history for the protoliths. The core to rim analyses of zircon grains in our study reveals an age zonation with 2.6–2.9 Ga cores showing oscillatory zoning mantled by 2.4 –2.5 Ga rims (cf. Fig. 4A). The cores of the zircons may thus record the age of emplacement of the magmas while the rims preserve the age of granulite facies metamorphism. Importantly, the rocks do not contain zircons with cores younger than 2.4 Ga, although a rounded zircon grain from garnet charnockite shows no core-rim age zonation and yields an age of ca. 3.2 Ga (Fig. 4C). This suggests that zircons from some older sources are present in the Madras Block.

Our results from the Madras Block also bring out the imprints of younger tectonothermal events on the rocks that were earlier considered to be of exclusively Archean age. An exception is the study by Miyazaki et al. (2000) who reported younger magmatic event from the

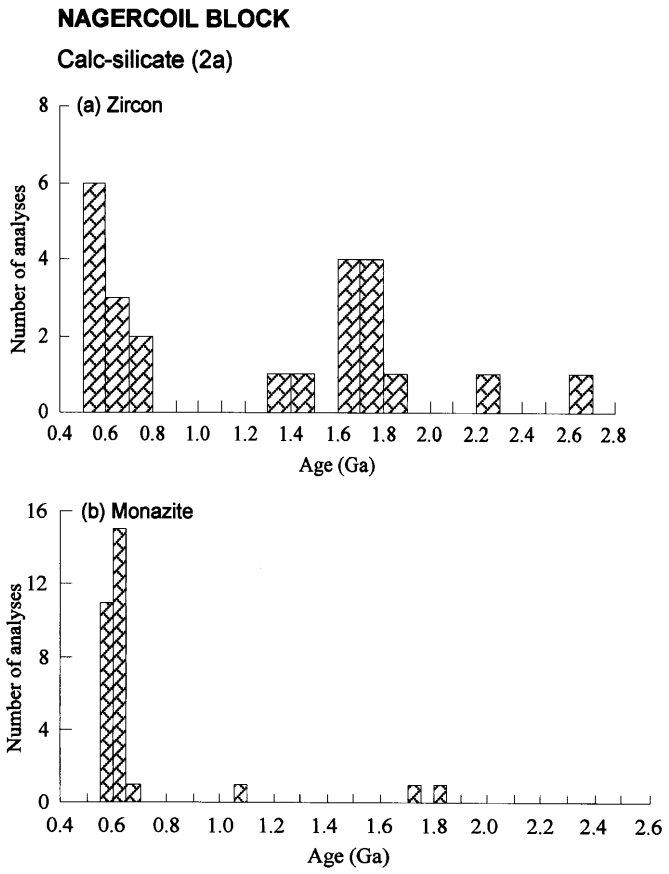

Fig. 15. Histograms showing compiled data from age values on zircon and monazite from the Nagercoil Block.

Madras Block. Local development of secondary ages on older zircons all recorded 1.7–2.4 Ga and such secondary overgrowths strongly suggest the thermal effect of a Paleo-Mesoproterozoic orogeny after Archean event.

Monazites from the Madras Block yield further interesting results. Both cores and rims of monazite in the charnockite sample yield ages around 2.3–2.5 Ga. The preservation of late Archean to earliest Proterozoic ages in monazites with no imprint of subsequent processes is important and indicates that monazite, in specific cases, could constitute a robust mineral for dating older events. Particularly when it occurs as inclusions within other minerals, the mineral is shielded from Pb loss during subsequent thermal events if the enclosing mineral is "inert" for Pb exchange with monazite. Minerals like garnet provide such an effective shield (cf. Montel et al., 1996). On the other hand, secondary zircon formed in metamict portions could result from lower temperatures, yielding ages younger than those from the monazite.

Madurai Granulite Block

Most of the samples and diverse rock types included in this study were from the Madurai Block, where a suite of 19 samples covered most of the dominant lithounits from the metamorphic and magmatic suites. Most of the minerals analysed (zircon, monazite, uraninite and huttonite) were also from this block, thus providing an exhaustive database for evaluating the tectonothermal history of this largest granulite block in southern India. The well-defined isochron plots from the gneiss, charnockite and granite bring out the salient results from the study. The gneiss yielded three isochrons at 1.7±0.1 Ga, 0.82±0.05 Ga and 0.58±0.04 Ga from core, inner rim and outer rim portions of zircon grains. These clearly defined isochrons bring out at least three major tectonothermal events in this block. Zircon grains from other samples in the metamorphic suite from this block also show peak core ages at 0.8–1.1 Ga. The data therefore suggest at least two major thermal events before late Pan-African event, one during the latest Paleoproterozoic and the other during the early Neoproterozoic. Several ages from secondary zircon overgrowths also converge at 0.75–0.92 Ga, indicating major rejuvenation/zircon growth at ca. 0.80 Ga. While the Paleo-Mesoproterozoic ages have been recorded in some previous studies from this block (1.85 Ga from zircon U–Pb analyses, Jayananda et al., 1995a), it is generally held that the peak metamorphism in the Madurai Block is of late Pan-African (553±15 Ma from Sm–Nd garnet whole-rock data, Jayananda et al., 1995a; 547±14 Ma from Pb ages by zircon evaporation, Bartlett et al., 1998). We show below that all these younger ages reported in previous studies represent subsequent thermal resetting, and do not correspond to the peak metamorphic age of the Madurai Block, which we place at ca. 0.8 Ga.

Zircons in pink metagranite represent the dominant magmatic phase in the Madurai Block and yield sharply defined isochrons of 0.68±0.03 Ga for the core and 0.57±0.01 Ga for the secondary (cf. Fig. 8). We interpret ca. 0.7 Ga as the emplacement age of the granite plutons. The 0.7 Ga event is also prominently reflected in zircon chronology from the metamorphic suite in this block, representing partial thermal resetting of those zircons during the magmatic event. The late Pan-African isochron age of 0.57 Ga from secondary overgrowth on zircons in the granite is identical with the 0.57 Ga isochron age for zircon rims in the orthogneiss sample that possess 1.7 Ga cores.

The late Pan-African ages from the Madurai Block are also widely represented in the monazite data. Monazite from metagranite shows 0.54–0.57 Ga cores and 0.51–0.52 Ga rims. Monazites from the metamorphic suite have 0.52–0.59 Ga core and 0.53–0.46 Ga rim. Uraninite from both metamorphic and magmatic suites has 0.54–0.51 Ga cores and 0.51–0.45 Ga rims. Huttonite from the orthogneiss possesses 0.54 Ga core and 0.51 Ga

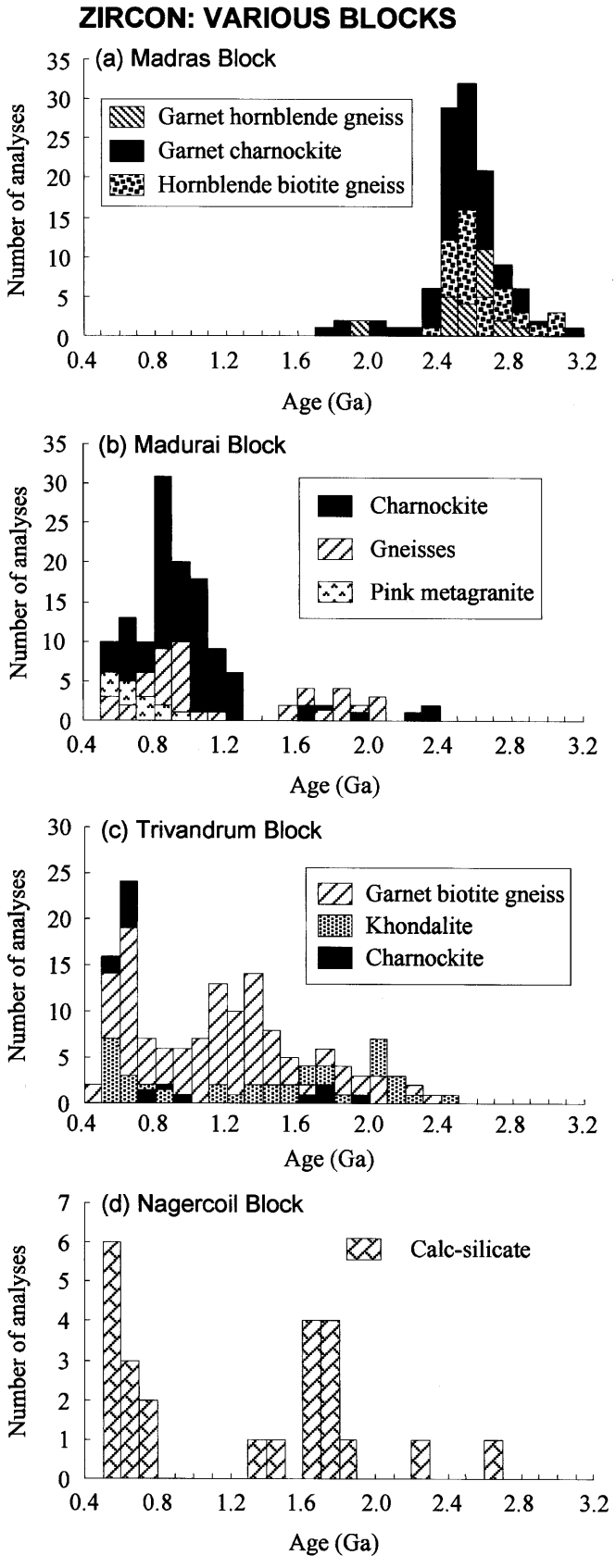

Fig. 16. Combined histograms showing age data on zircons from various granulite blocks in southern India.

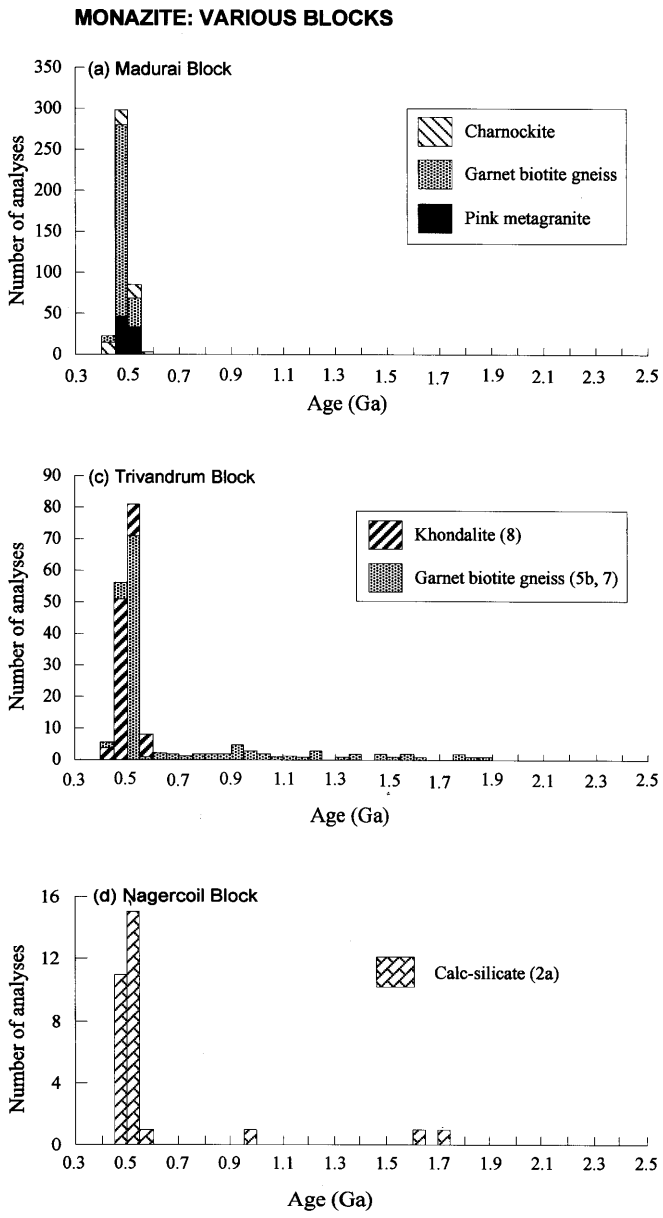

Fig. 17. Combined histograms showing age data on monazites from the various granulite blocks in southern India.

rims. No older monazites occur in any of these rocks, suggesting that monazite in this block mostly formed at this time. It is to be noted that previous studies in the Madurai Block recorded mostly Pan-African ages only, relating the high-grade metamorphism in this block to late Pan-African time (cf. Jayananda et al., 1995a). However, our data does not preclude the possibility of an earlier thermal event that caused re-melting of older crust close to 1.8 Ga.

All the late Pan-African ages in the Madurai Block are identical to those in the Trivandrum and Nagercoil Blocks that occur to the south (see next section), and could, therefore, be thermal overprints. Pre - Pan-African events

in the Madurai and Trivandrum Blocks have been recently discussed by Yoshida et al. (2000). Our study shows that the major tectonothermal event in the Madurai Block is between 0.8–1.0 Ga with peak at ca. 0.8 Ga, in total contrast to the peak ages obtained from the Madras Block to the north (excluding the ca. 0.8 Ga ages reported from two syenite plutons in the Madras Block by Miyazaki et al., 2000), as well as the Trivandrum and Nagercoil Blocks to the south (see below). This finding suggests an "exotic" status for the Madurai Block in the Proterozoic terrain collage of southern India.

Trivandrum and Nagercoil Granulite Blocks

The late Pan-African tectonothermal event is substantiated by monazite data from both the Trivandrum and Nagercoil Blocks. Older relic monazites were also obtained from both blocks in our study, confirming previous works by Bindu (1998), Bindu et al. (1998) and Braun et al. (1998). This major late Pan-African tectonothermal event led to the growth only on zircon rims. Ages of the zircon cores are various up to 2.8 Ga, indicating a mixed provenance that may include Archean source regions. The presence of detrital monazite with 0.7 Ga shows that some metamorphic rocks in the blocks were derived from sandstones deposited more recently than 0.7 Ga.

Terrain assembly

Our study confirms the proposal that the Palghat-Cauvery Shear Zone could mark a major terrain boundary between an Archean craton in the north and Proterozoic terrains in the south (Harris et al., 1994). It also strengthens the proposal of Paleoproterozoic accretion and Pan-African reworking in the southern granulite blocks (Santosh, 2000). Some of the crust in these accreted terrains may have been juvenile at the time of accretion, but many of the ages have apparently been imposed on older crust. However, evidence for large-scale accretion of new crust during Paleoproterozoic is yet to be identified, and the available Nd isotope data mostly suggest reworking of Archean crust during Paleoproterozoic with only a limited addition of juvenile crust. Available Nd isotope data provides only limited evidence for the accretion of new crust.

Among the four blocks included in this study, the peak ages for zircon and monazite crystallization during late Archean is seen in rocks from the Madras Block. Although these rocks and their protoliths appear to be predominantly late Archean, the presence of a minor older component is also identified from grains with 3.2 Ga age. In contrast, ages older than Paleoproterozoic in the southern blocks, are restricted to detrital grains. Thus, the terrains south of the Palghat-Cauvery Shear Zone were apparently accreted on the Archean craton subsequent to the major tectonothermal event in the northern block.

One of the most important findings in our study is the presence of 1.5–1.8 Ga ages with peak at 1.7 Ga in all the granulite blocks. These ages are particularly dominant in the block south of the Palghat-Cauvery Shear Zone. Although previous studies (e.g., Jayananda et al., 1995a; Bartlett et al., 1988; Bindu et al., 1988) detected Paleoproterozoic ages of ca. 1.8 Ga in some suites from the Madurai and Trivandrum Blocks, our study is the first to systematically detect and clearly constrain this older age from terrains that have been re-worked by younger tectonothermal events. The fact that the major granulite block in general, and the Proterozoic terrains in particular, preserve this Paleo-Mesoproterozoic memory has important implications on supercontinent history, as discussed in a subsequent section.

The dominant cluster of ages from the metamorphic suite in the Madurai Block at around 0.8 Ga is absent both in the Madras Block to the north and the Trivandrum and Nagercoil blocks to the south. Granite magmatism in the Madurai Block is dated at around ca. 0.7 Ga. Several late Pan-African ages (ca. 0.6–0.5 Ga) are present in monazites and zircon rims in this block, identical to the late Pan-African metamorphic event assigned to this block in previous studies (e.g., Jayananda et al., 1995a). Igneous texture is preserved only in rocks formed after the major thermal event at ca. 0.8 Ga. The distribution of ages in the Madurai Block provides absolute dates for events that have been recognized but undated in previous studies. A principal one is careful petrologic and phase equilibria studies (e.g., Raith et al., 1997; Sajeev et al., 2001) that show an early ultrahigh-temperature metamorphism followed by isobaric cooling and a subsequent isothermal decompression. Although the samples dated in this study are not those on which the above petrologic inferences have been drawn, a tentative correlation of our data would assign the ultrahigh-temperature metamorphism to the 1.7 Ga event and subsequent isothermal uplift at 0.8 Ga. Apparently, this ultrahigh-temperature metamorphism was not sufficiently intense and widespread to reset ages as old as 2.5 Ga in some zircons of the Madurai Block.

The late Pan-African ages in the Madurai Block could be overprints from the strong late Pan-African orogeny in the Trivandrum and Nagercoil Blocks, which fall along a proposed Pan-African suture linking East African Orogen from the Mozambique belt through Madagascar and India, extending into East Antarctica (cf. Jacobs et al., 1998; Santosh and Yoshida, 2001). This might suggest that the Trivandrum and Nagercoil Blocks were not amalgamated with the Madurai Block at least until 800 Ma. The

proposed suture is supported by the presence of detrital monazites with ca. 0.7 Ga in the Trivandrum and Nagercoil Blocks, with final terrain assembly along the Achankovil Shear Zone in the late Pan-African, coinciding with the birth of Gondwana.

Implications on Supercontinent History

The ages of production, accretion, and reworking in the terrains of southern India yield important information for the history of three supercontinents. Columbia was proposed by Rogers and Santosh (2002) to have begun accretion at ~1.9–1.8 Ga, reach maximum packing at 1.6–1.5 Ga, and begin rifting at 1.5 Ga. An alternative configuration of Columbia was proposed by Zhao et al. (2002). Rodinia developed during Grenville-age orogenies at ~1.1–1.0 Ga and began rifting at ~750 Ma. Numerous configurations of Rodinia have been proposed, including those by Hoffman (1991), Rogers (1996), Karlstrom et al. (1999), Meert (2001), and Wingate et al. (2002). A supercontinent of the same age is referred to as Palaeopangaea by Piper (2001). Gondwana developed during the Pan-African/Brasiliano orogeny at ~0.6–0.5 Ga, when East and West Gondwana fused along a suture whose location is highly controversial.

Accretion of Columbia occurred at the same time as accretion of reworked and/or juvenile terrains of the Madurai Block to Archean India (Fig. 18a). The Madurai

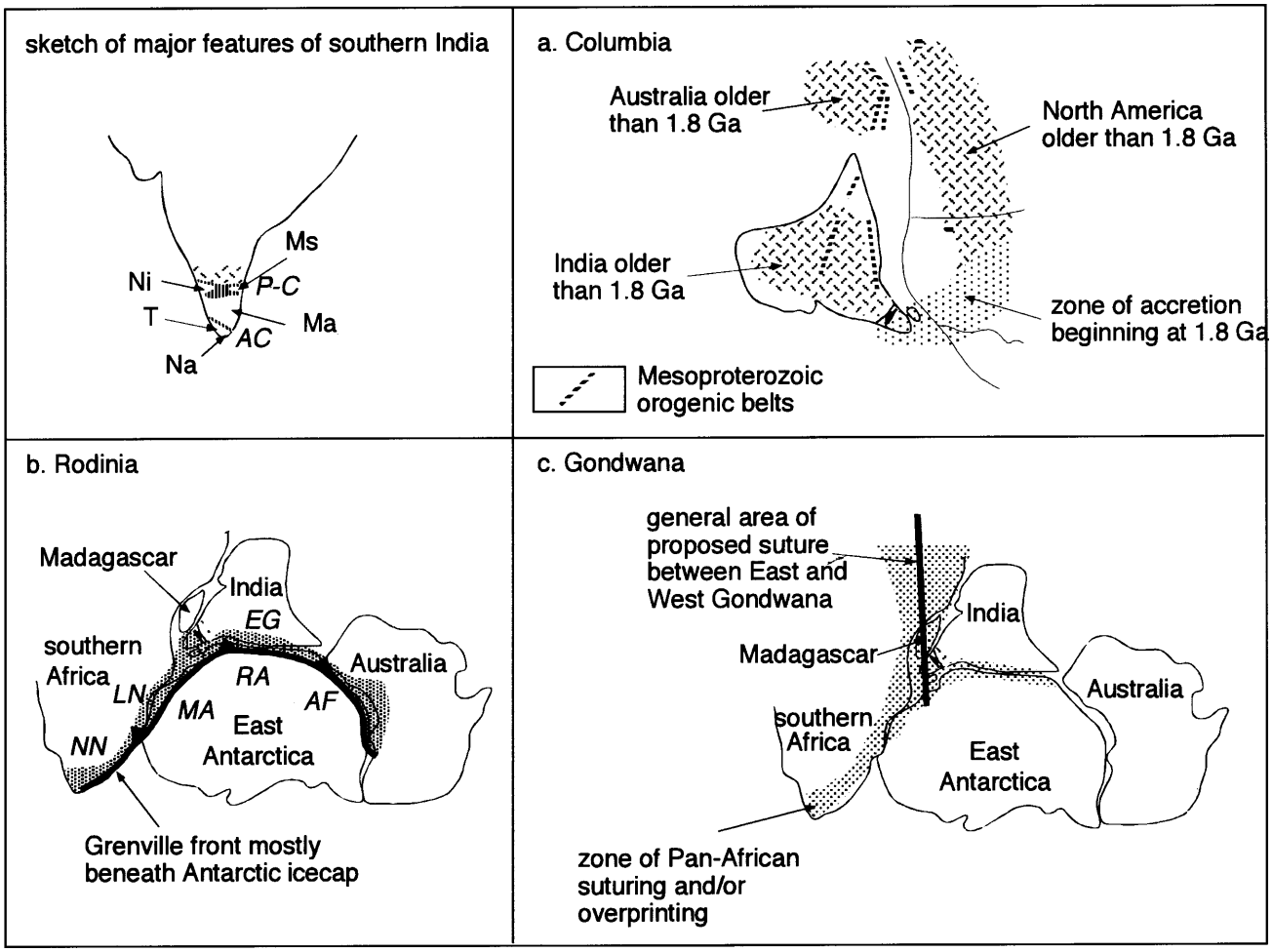

Fig. 18. Relationship of southern India to three supercontinents. Sketch map: P-C–Palghat-Cauvery Shear Zone, AC–Achankovil Shear Zone, Ms–Madras Block, Ni–Nilgiri Block, Ma–Madurai Block, T–Trivandrum Block, Na–Nagercoil Block. (a) Columbia: Map shows regions of India, western Australia, and western North America stabilized before 1.8 Ga. Linear Mesoproterozoic orogenic belts have a lined pattern. Accretion to southwestern North America began at approximately the same time as accretion of the Madurai block. (b) Rodinia: Shaded area shows extent of Grenville-age orogeny and thermal activity. All vergences are shown by triangles as away from East Antarctica, indicating the front is somewhere beneath the Antarctic icecap. Southern India is farther away from the front than other areas that contain Grenville ages. Principal orogenic belts are: NN–Namaqua-Natal, LN–Lurio-Namama, MA–Maudheim, RA–Rayner, EG–Eastern Ghats, AF–Albany-Fraser. (c) Gondwana: Zone of Pan-African suturing and/or overprinting is shaded. Proposed suture from eastern Africa to East Antarctica extends through southern India.

Block appears to be part of the worldwide network of orogenic belts that is centered around 1.8 Ga and outlines the configuration of Columbia as proposed by Rogers and Santosh (2002). Accretion of terrains in the Madurai Block to Archean rocks north of the Palghat-Cauvery Shear Zone at this time is consistent with the ages suggested to be the oldest metamorphic event in the Eastern Ghats orogen of eastern India and the Rayner belt of coastal East Antarctica (cf. Rogers and Santosh, 2002). In contrast to the accretion in the Madurai Block, however, there is no present information that distinguishes between accretion and overprinting of older rocks in the Eastern Ghats and Rayner belts at ~1.8 Ga, but intense overprinting at ~1 Ga and ~0.5 Ga make it difficult to interpret these older ages.

Involvement of southern India in the accretion of Rodinia is unclear (Fig. 18b). Yoshida et al. (2000) interpreted the scatter of ages between 1.2–0.8 Ga in some of the southern Indian granulite blocks as the strong imprint of rejuvenation at 0.8 Ga of an earlier Grenville orogeny. However, none of the rocks in southern India show the clear effect of the Grenville-age orogenies at ~1.1–1 Ga, but ages from 1.0–0.8 Ga are common in the Madurai Block, which underwent its major metamorphic event at ~0.8 Ga. Grenville ages are common, however, in the Eastern Ghats Belt and correlate with similar ages in the southern margin of the Kalahari Block of Africa, along the southern margin of Australia, and throughout the coastal region of East Antarctica. Apparently at the time that Rodinia was assembled, the granulite terrane of southern India was far enough away from the Grenville accretionary belt that it was largely unaffected by the orogeny, suggesting that the 0.8 Ga event in the Madurai Block represents thermal relaxation following the principal collision. The absence of 1.1–1.0 Ga ages also suggests that the Grenville-age suture was far to the south (present orientation) of India, presumably now buried under the East Antarctic icecap.

Data in this paper confirm earlier evidence that all of southernmost India underwent resetting of isotopic systems during the final accretion of Gondwana at the time of the Pan-African orogeny at ~0.5 Ga (Fig. 18c). This is consistent with evidence of intense Pan-African thermal activity and left-lateral shearing along the eastern margin of Africa, through Madagascar, and into a contiguous part of East Antarctica. The possibility that the Trivandrum and Nagercoil terrains accreted to the Madurai Block after ~0.8 Ga suggests that this Pan-African zone may have been a suture that involved the closure of ocean basins, although alternate models have also been considered in some recent works (e.g., Yoshida et al., 2002). Our interpretation is consistent with proposals that the Achankovil and related shears in other continents were the principal zone of suturing between East and West Gondwana (Shackleton, 1996; Jacobs et al., 1998; Santosh and Yoshida, 2001; Collins and Windley, 2002). Conversely, similar histories of older events in the Madurai and Trivandrum Blocks may indicate that the Achankovil Zone is an intracontinental shear, with suturing and closure of ocean basins occurring elsewhere in Gondwana.

Acknowledgments

M. Santosh thanks Dr. K.R. Gupta, Advisor (ESS), DST, Government of India, for support during the early part of this work, and Prof. S. Yoshikura for valuable encouragement. We greatly appreciate constructive reviews from Dr. M. Jayananda and Prof. M. Yoshida on an earlier version of this paper.

References

Bartlett, J.M., Harris, N.B.W., Hawkesworth, C.J. and Santosh, M. (1995) New isotope constraints on the crustal evolution of southern India. Geol. Soc. India, Mem. No. 34, pp. 391-397.

Bartlett, J.M., Dougherty-Page, J.S., Harris, N.B.W., Hawksworth, C.J. and Santosh, M. (1998) The application of single zircon evaporation and model Nd ages to the interpretation of polymetamorphic terrains: an example from the Proterozoic mobile belt of South India. Contrib. Mineral. Petrol., v. 131, pp. 181-195.

Bernard-Griffiths, J., Jahn, B-M. and Sen, S.K. (1987) Sm–Nd isotopes and REE geochemistry of Madras granulites, India: an introductory statement. Precamb. Res., v. 37, pp. 343-355.

Biju-Sekhar, S., Pandit, M.K., Yokoyama, K. and Santosh, M. (2002) Electron microprobe dating of the Ajitgarh and Barodiya granitoids, NW India: implications on the evolution of Delhi fold belt. J. Geosci., Osaka City Univ., v. 45, pp. 13-27.

Bindu, R.S. (1998) Geochronological study of Precambrian terrains of South India and surrounding Gondwana areas-first attempt on electron microprobe chemical U–Pb–Th method. D. Sc. Thesis (unpub.), Osaka City Univ., 131p.

Bindu, R.S., Yoshida, M. and Santosh, M. (1997) Electron microprobe dating of monazite from Chittikara granulite, South India. Evidence for polymetamorphic events. J. Geosci., Osaka City Univ., v. 41, pp. 77-83.

Bindu, R.S., Suzuki, K., Yoshida, M. and Santosh, M. (1998) The first report of CHIME monazite age from the South Indian granulite terrain. Curr. Sci., v. 74, pp. 852-858.

Brandon, A.D. and Meen, J.K. (1995) Nd isotopic evidence for the position of southernmost Indian terranes within East Gondwana. Precamb. Res., v. 37, pp. 343-355.

Braun, I., Montel, J. and Nicollet, C. (1998) Electron microprobe dating of monazites from high-grade gneisses and pegmatites of the Kerala Khondalite Belt, southern India. Chem. Geol., v. 146, pp. 65-85.

Chacko, T., Lamb, M. and Farquhar, J. (1996) Ultra high temperature metamorphism in the Kerala Khondalite Belt. In: Yoshida, M. and Santosh, M. (Eds.), The Archaean and Proterozoic terrains in southern India within East Gondwana. Gondwana Res. Group Mem. No. 3, Field Sci. Publ., Osaka, pp. 157-165.

Chacko, T., Ravindra Kumar, G.R. and Newton, R.C. (1987) Metamorphic P-T conditions of the Kerala (South India) Khondalite Belt, a granulite facies supracrustal terrain. J. Geol., v. 95, pp. 343-358.

Chaudhary, A.K., Harris, N.B.W., Van Calsteran, P. and Hawkesworth, C.J. (1992) Pan-African charnockite formation in Kerala, South India. Geol. Mag., v. 129, pp. 257-264.

Cherniak, D.J., Lanford, W.A. and Ryerson, F.J. (1991) Lead diffusion in apatite and zircon using ion implantation and Rutherford back scattering techniques. Geochim. Cosmochim. Acta, v. 55, pp. 1663-1673.

Collins, A.S. and Windley, B.F. (2002) The tectonic evolution of Central and northern Madagascar and its place in the final assembly of Gondwana. J. Geol., v. 110, pp. 325-339.

Crawford, A.R. (1969) India, Ceylon and Pakistan new age data and comparison, Nature, v. 223, pp. 380-384.

Drury, S.A. and Holt, R.W. (1980) The tectonic framework of South India: a reconnaisance involving LANDSAT imagery. Tectonophys., v. 65, pp. 1-15.

Hansen, E.C., Hickman, M.H., Grant, N.K. and Newton, R.C. (1985) Pan-African age of peninsular gneiss near Madurai, South India. EOS, v. 66, pp. 419-420.

Hanchar, J.M. and Miller, C.F. (1993) Zircon zonation patterns as revealed by cathodoluminesence and back scattered electron images: implications for interpretation of complex crustal histories. Chem. Geol., v. 110, pp. 1-13.

Harris, N.B.W., Bartellat, J.M. and Santosh, M. (1996) Neodymium isotope constraints on the tectonic evolution of East Gondwana. J. Southeast Asian Earth Sci., v. 14, pp. 119-125.

Harris, N.B.W., Santosh, M. and Taylor, P.N. (1994) Crustal evolution in South India: constraints from Nd isotopes. J. Geol., v. 102, pp. 139-150.

Hoffman, P.F. (1991) Did the breakout of Laurentia turn Gondwanaland inside out? Science, v. 252, pp. 1409-1412.

Holmes, A. (1931) Radioactivity and geological time. National Research Council, Bull. No. 80, pp. 24-459.

Jacobs, J., Fanning, C.M., Henjes-Kunst, F., Olesch, M. and Paech, H.J. (1998) Continuation of the Mozambique belt into East Antarctica: Greenville-age metamorphism and polyphase Pan-African high-grade events in Central Dronning Maud Land. J. Geol., v. 106, pp. 385-406.

Jayananda, M. and Peucat, J.-J. (1995) Archaean crust formation in southern India: geochronologic and isotopic constraints. In: Yoshida, M., Santosh, M. and Rao, A.T. (Eds.), India as a fragment of East Gondwana. Gondwana Res. Group Mem. No. 2, Field Sci. Publ., Osaka, pp. 15-21.

Jayananda, M. and Peucat, J.-J. (1996) Geochronological framework of southern India. In: Santosh, M. and Yoshida, M. (Eds.), The Archaean and Proterozoic terrains in southern India within East Gondwana. Gondwana Res. Group Mem. No. 3, Field Sci. Publ., Osaka, pp. 53-75.

Jayananda, M., Janardhan, A.S., Sivasubramanian, P. and Peucat, J.-J. (1995a) Geochronologic and isotopic constraints on the granulite formation in the Kodaikanal area, southern India. In: Yoshida, M. and Santosh, M. (Eds.), India and Antarctica during Precambrian. Geol. Soc. India, Mem. No. 34, pp. 373-390.

Jayananda, M., Martin, H., Peucat, J.-J. and Mahabaleshwar, B. (1995b) The late Archaean crust-mantle interactions: geochemistry of LREE enriched mantle derived magmas-the closepet batholith of southern India. Contrib. Mineral. Petrol., v. 119, pp. 314-329.

Jayananda, M., Moyen, J.F., Martin, H., Peucat, J.-J., Auvrey, B. and Mahabaleswar, B. (2000) Late Archaean (2550–2520 Ma) juvenile magmatism in the eastern Dharwar Craton, southern India: constraints from geochronology, Nd–Sr isotopes and whole-rock geochemistry. Precamb. Res., v. 99, pp. 225-254.

Karlstrom, K.E., Harlan, S.S., Williams, M.L., McLelland, J., Geissman, J.W. and Ahall, A.-I. (1999) Refining Rodinia: geologic evidence for the Australia-western U.S. connection. GSA Today, v. 9, No. 10, pp. 1-7.

Meen, J.K., Rogers, J.J.W. and Fullagar, P.D. (1992) Pb isotopic compositions of the Western Dharwar Craton, southern India: evidence for distinct Middle Archean terranes in a late Archean craton. Geochim. Cosmochim. Acta, v. 56, pp. 2455-2470.

Meert, J.G. (2001) Growing Gondwana and refining Rodinia: a paleomagnetic perspective. Gondwana Res., v. 4, pp. 279-288.

Menon, R.D., Santosh, M. and Yoshida, M. (1994) Gemstone mineralisation in southern Kerala, India. J. Geol. Soc. India, v. 44, pp. 241-252.

Miller, J.S., Santosh, M., Pressley, R.A., Clements, A.S. and Rogers, J.J.W. (1996) A Pan-African thermal event in southern India. J. Southeast Asian Earth Sci., v. 14, pp. 127-136.

Miyazaki, T., Kagami, H., Shuto, K., Morikiyo, T., Ram Mohan, V. and Rajasekaran, K.C. (2000) Rb–Sr geochronology, Nd–Sr isotopes and whole-rock geochemistry of Yelagiri and Sevattur syenites, Tamil Nadu, South India. Gondwana Res., v. 3, pp. 39-53.

Mohan, A. and Jayananda, M. (1999) Metamorphism and isotopic evolution of granulites of southern India: reference to Neoproterozoic crustal evolution. Gondwana Res., v. 2, pp. 251-262.

Mohan, A. and Windley, B.F. (1993) Crustal trajectory of sapphirine-bearing granulites from Ganguvarpatti, South India: evidence for isothermal decompression path. J. Metam. Geol., v. 11, pp. 867-878.

Montel, J.M., Foret, S., Veschambre, M., Nicollet, C. and Provost, A. (1996) Electron microprobe dating of monazite. Chem. Geol., v. 131, pp. 37-53.

Parrish, R.R. (1990) U–Pb dating of monazite and its applications to geological problems. Can. J. Earth Sci., v. 27, pp. 1431-1450.

Peucat, J.-J., Vidal, P., Bernard-Griffiths, J. and Condie, K.C. (1989) Sr, Nd and Pb isotopic systematics in the Archaean low- to high-grade transition zone in southern India: synaccretion vs. post accretion granulites. J. Geol., v. 97, pp. 537-550.

Piper, J.D.A. (2001) The Neoproterozoic supercontinent: Rodinia or Palaeopangaea? Earth Planet. Sci. Lett., v. 176, pp. 131-146.

Radhakrishna, B.P. (1989) Suspect tectono-stratigraphic terrane elements in the Indian subcontinent. J. Geol. Soc. India, v. 34, pp. 1-24.

Raith, M., Karmakar, S. and Brown, M. (1997) Ultra-high temperature metamorphism and multistage decompressional evolution of sapphirine granulites from the Palni Hill Ranges, southern India. J. Metam. Geol., v. 15, pp. 379-399.

Raith, M., Srikantappa, C., Buhl, D. and Koehler, H. (1999) The Nilgiri enderbites, South India: nature and age constraints on protolith formation, high-grade metamorphism and cooling history. Precamb. Res., v. 98, pp. 129-150.

Rogers, J.J.W. (1996) A history of continents in the past three billion years. J. Geol., v. 104, pp. 91-107.

Rogers, J.J.W. and Santosh, M. (2002) Configuration of Columbia, a Mesoproterozoic supercontinent. Gondwana Res., v. 5, pp. 5-22.

Sajeev, K., Osanai, Y. and Santosh, M. (2001) Ultrahigh-temperature stability of sapphirine and kornerupine in Ganguvarpatti granulite, Madurai Block, southern India. Gondwana Res., v. 4, pp. 762-766.

Santosh, M. (1987) Cordierite gneisses of southern Kerala, India: petrology, fluid inclusions and implications for crustal uplift history. Contrib. Mineral. Petrol., v. 96, pp. 343-356.

Santosh, M. (2000) Palaeoproterozoic accretion, Pan-African reworking and fluid-driven processes in the continental deep crust in southern India. Indian Mineral., v. 34, pp. 22-28.

Santosh, M. and Yoshida, M. (2001) Pan-African extensional collapse along the Gondwana suture. Gondwana Res., v. 4, pp. 188-191.

Santosh, M., Harris, N.B.W., Jackson, D.H. and Mattey, D.P. (1990) Dehydration and incipient charnockite formation: a phase equilibria and fluid inclusion study from South India. J. Geol., v. 98, pp. 915-926.

Santosh, M., Kagami, H., Yoshida, M. and Nandakumar, V. (1992) Pan-African charnockite formation in East Gondwana: geochronologic (Sm–Nd and Rb–Sr) and petrogenetic constraints. Indian Geol. Assoc. Bull., v. 25, pp. 1-10.

Santosh, M., Tagawa, M., Taguchi, S. and Yoshikura, S. (2002) The Nagercoil granulite block, southern India: petrology, fluid inclusions and exhumation history. J. Asian Earth Sci., (in press).

Satish-Kumar, M., Wada, H. and Santosh, M. (2002) Constraints on the application of carbon isotope thermometry in high- to ultrahigh-temperature metamorphic terranes. J. Metam. Geol., v. 20, pp. 335-350.

Semenov, E. and Santosh, M. (1997) Rare metal mineralization in alkaline pegmatites of southern Indian granulite terrain. Gondwana Res., v. 1, pp. 152-153.

Shackleton, R.M. (1996) The final collision zone between East and West Gondwana: where is it? J. Afr. Earth Sci., v. 23, pp. 271-287.

Soman, K., Nair, N.G.K., Golubyev, V.N. and Arakelyan, M.M. (1982) Age data on pegmatites of South Kerala and their tectonic significance. J. Geol. Soc. India, v. 23, pp. 458-462.

Srikantappa, C. (1996) The Nilgiri granulites. In: Santosh, M. and Yoshida, M. (Eds.), The Archaean and Proterozoic terrains of southern India within East Gondwana. Gondwana Res. Group Mem. No. 3, pp. 185-222.

Srikantappa, C., Raith, M. and Spiering, B. (1985) Progressive charnockitization of a leptynite-khondalite suite in southern Kerala, India: evidence for formation of charnockites through a decrease in fluid pressure? J. Geol. Soc. India, v. 26, pp. 62-83.

Steiger, R.H. and Jäger, E. (1977) Subcommission on geochronology: convention on the use of decay constants in geo- and cosmochronology. Earth Planet. Sci. Lett., v. 36, pp. 359-362.

Suzuki, K. and Adachi, M. (1991) Precambrian provenance and Silurian metamorphism of the Tsubonosawa paragneiss in the South Kitakami terrane, northeast Japan, revealed by the chemical Th–U-total Pb isochron ages of monazite, zircon and xenotime. J. Geochem., v. 25, pp. 357-376.

Suzuki, K. and Adachi, M. (1994) Middle Precambrian detrital monazite and zircon from the Hida gneiss on Oki-Dogo Island, Japan: their origin and implications for the correlation of basement gneiss of southwest Japan and Korea. Tectonophys., v. 235, pp. 277-292.

Suzuki, K., Adachi, M. and Tanaka, T. (1991) Middle Precambrian provenance of Jurassic sandstone in the Mino terrane, Central Japan: Th–U-total Pb evidence from an electron microprobe monazite study. Sediment. Geol., v. 75, pp. 141-147.

Unnikrishnan-Warrier, C., Santosh, M. and Yoshida, M. (1995) First report of Pan-African Sm–Nd and Rb–Sr mineral isochron ages from regional charnockites of southern India. Geol. Mag., v. 132, pp. 253-260.

Vinogradov, A., Tugarinov, A., Zhycov, C., Stapnikova, N., Bibikova, E. and Khorre, K. (1964) Geochronology of the Indian Precambrian. XXII Intl. Geol. Cong. Rep., pp. 553-567.

Windley, B.F., Razafiniparany, A., Razakamanana, T. and Ackermand, D. (1994) Tectonic framework of the Precambrian of Madagascar and its Gondwana connections: a review and reappraisal. Geol. Rundschau, v. 83, pp. 642-659.

Wingate, M.T.D., Pisarevsky, S.A. and Evans, D.A.D. (2002) Rodinia connections between Australia and Laurentia: no SWEAT, no AUSWUS? Terra Nova, v. 14, pp. 121-128.

York, D. (1966) Least-squares fitting of a straight line. Can. J. Phys., v. 44, pp. 1079-1088.

Yoshida, M., Santosh, M. and Arima, M. (2000) Pre-Pan African and Pan-African events in South India and their implications for Gondwana tectonics. Geol. Surv. India, Spl. Publ. No. 57, pp. 9-25.

Yoshida, M., Jacobs, J., Santosh, M. and Rajesh, H.M. (2002) Role of Pan-African events in the Circum East Antarctic Orogen of East Gondwana: a critical overview. Geol. Soc. London, Spl. Publ. (in press).

Yoshida, M., Bindu, R.S., Kagami, H., Rajesham, T., Santosh, M. and Shirahata, H. (1996) Geochronologic constraints on granulite facies terranes of South India and their implications for the Precambrian assembly of Gondwana. J. Southeast Asian Earth Sci., v. 14, pp. 137-147.

Zhao, G., Cawood, P.A., Wilde, S.A. and Sun, M. (2002) Review of global 2.1–1.8 Ga collisional orogens and accreted cratons: a pre-Rodinia supercontinent? Earth Sci. Rev. (in press).

Appendix

Table A-1. EPMA analyses of zircons from the Madras Block.

UO_2 (wt.%)	ThO_2 (wt.%)	PbO (wt.%)	Age (Ga)	ThO_2* (wt.%)	UO_2 (wt.%)	ThO_2 (wt.%)	PbO (wt.%)	Age (Ga)	ThO_2* (wt.%)
Garnet hornblende gneiss (47/4)					*Garnet charnockite (49/1) Contd.*				
0.142	0.204	0.094	2.660	0.793	0.111	0.009	0.052	2.526	0.461
0.128	0.068	0.072	2.660	0.602	0.105	0.021	0.052	2.560	0.453
0.097	0.063	0.054	2.595	0.464	0.116	0.017	0.052	2.407	0.482
0.090	0.070	0.051	2.608	0.442	0.108	0.009	0.051	2.532	0.449
0.083	0.081	0.050	2.628	0.423	0.103	0.007	0.049	2.543	0.430
0.075	0.108	0.045	2.483	0.412	0.075	0.065	0.048	2.813	0.383
0.079	0.093	0.045	2.449	0.413	0.093	0.000	0.046	2.641	0.387
0.072	0.060	0.042	2.651	0.357	0.069	0.075	0.045	2.734	0.366
0.068	0.065	0.042	2.695	0.351	0.063	0.062	0.043	2.880	0.334
0.062	0.054	0.042	2.879	0.322	0.095	0.018	0.043	2.427	0.400
0.070	0.054	0.040	2.643	0.343	0.068	0.026	0.043	2.945	0.322
0.063	0.058	0.035	2.498	0.315	0.075	0.011	0.042	2.799	0.332
0.076	0.006	0.035	2.500	0.313	0.081	0.021	0.041	2.562	0.355
0.057	0.049	0.032	2.524	0.282	0.086	0.000	0.040	2.540	0.352
0.052	0.047	0.030	2.590	0.261	0.057	0.069	0.039	2.820	0.312
0.050	0.043	0.030	2.642	0.251	0.069	0.045	0.039	2.645	0.330
0.046	0.044	0.029	2.733	0.237	0.057	0.014	0.039	3.156	0.270
0.049	0.057	0.029	2.515	0.256	0.071	0.029	0.038	2.609	0.322
0.046	0.039	0.028	2.677	0.231	0.056	0.062	0.035	2.642	0.294
0.040	0.039	0.025	2.686	0.205	0.063	0.028	0.032	2.549	0.285
0.038	0.030	0.022	2.613	0.186	0.055	0.050	0.032	2.566	0.276
0.035	0.020	0.021	2.759	0.167	0.058	0.000	0.029	2.696	0.243
0.046	0.000	0.020	2.428	0.184	0.050	0.013	0.026	2.640	0.218
0.086	0.079	0.035	1.986	0.405	0.042	0.036	0.025	2.642	0.210
0.061	0.051	0.025	1.988	0.284	0.037	0.023	0.021	2.696	0.177
Garnet charnockite (49/1)					*Garnet charnockite (54/3)*				
0.099	0.000	0.034	2.022	0.380	0.248	0.006	0.115	2.542	1.018
0.133	0.000	0.046	2.040	0.508	0.172	0.000	0.083	2.623	0.712
0.111	0.006	0.034	1.824	0.420	0.180	0.000	0.083	2.537	0.737
0.104	0.012	0.032	1.804	0.401	0.108	0.000	0.051	2.565	0.442
0.135	0.010	0.039	1.737	0.508	0.088	0.006	0.049	2.867	0.384
0.104	0.034	0.042	2.186	0.440	0.082	0.000	0.048	2.961	0.357
0.534	0.031	0.252	2.551	2.219	0.095	0.000	0.047	2.640	0.395
0.460	0.014	0.209	2.494	1.882	0.106	0.000	0.046	2.416	0.425
0.265	0.013	0.124	2.534	1.096	0.093	0.000	0.045	2.607	0.385
0.217	0.000	0.101	2.558	0.888	0.086	0.018	0.045	2.669	0.375
0.188	0.000	0.089	2.594	0.773	0.075	0.031	0.044	2.778	0.349
0.171	0.000	0.086	2.686	0.714	0.084	0.011	0.039	2.509	0.352
0.180	0.008	0.085	2.551	0.746	0.085	0.011	0.039	2.451	0.353
0.174	0.014	0.084	2.590	0.730	0.082	0.000	0.038	2.557	0.336
0.190	0.000	0.084	2.459	0.766	0.068	0.000	0.037	2.800	0.291
0.121	0.137	0.081	2.771	0.649	0.067	0.000	0.036	2.783	0.286
0.161	0.000	0.078	2.617	0.664	0.061	0.027	0.034	2.690	0.281
0.160	0.010	0.073	2.477	0.660	0.067	0.000	0.033	2.621	0.279
0.148	0.000	0.071	2.597	0.611	0.060	0.008	0.032	2.728	0.260
0.148	0.011	0.070	2.539	0.616	0.069	0.000	0.032	2.510	0.283
0.144	0.000	0.067	2.561	0.591	0.054	0.022	0.031	2.769	0.248
0.145	0.009	0.066	2.481	0.597	0.060	0.000	0.031	2.724	0.253
0.150	0.000	0.066	2.440	0.606	0.065	0.000	0.029	2.456	0.264
0.123	0.014	0.064	2.692	0.529	0.057	0.007	0.028	2.622	0.242
0.117	0.069	0.063	2.580	0.550	0.053	0.011	0.028	2.678	0.231
0.140	0.000	0.062	2.453	0.565	0.055	0.008	0.027	2.567	0.233
0.133	0.017	0.061	2.469	0.557	0.047	0.030	0.026	2.568	0.224
0.138	0.006	0.060	2.408	0.559	0.057	0.000	0.025	2.421	0.229
0.127	0.000	0.059	2.526	0.520	0.047	0.015	0.024	2.593	0.210
0.129	0.022	0.059	2.429	0.542	0.037	0.025	0.024	2.869	0.184
0.118	0.000	0.057	2.608	0.488	0.047	0.000	0.024	2.695	0.195
0.082	0.072	0.053	2.806	0.420	0.045	0.008	0.021	2.443	0.191

Table A-1. *Contd.*

UO_2 (wt.%)	ThO_2 (wt.%)	PbO (wt.%)	Age (Ga)	ThO_2* (wt.%)	UO_2 (wt.%)	ThO_2 (wt.%)	PbO (wt.%)	Age (Ga)	ThO_2* (wt.%)
Garnet charnockite (54/3) Contd.					*Hornblende biotite gneiss (54/1) Contd.*				
0.047	0.000	0.021	2.454	0.188	0.058	0.014	0.031	2.712	0.256
0.045	0.000	0.021	2.534	0.182	0.046	0.045	0.031	2.846	0.242
0.290	0.034	0.127	2.391	1.194	0.055	0.021	0.031	2.730	0.251
0.142	0.030	0.066	2.461	0.606	0.045	0.009	0.029	3.041	0.210
0.133	0.000	0.059	2.480	0.538	0.046	0.020	0.029	2.906	0.220
0.119	0.035	0.055	2.404	0.511	0.041	0.034	0.027	2.879	0.210
0.079	0.038	0.036	2.290	0.351	0.047	0.038	0.027	2.586	0.232
0.056	0.040	0.028	2.373	0.265	0.053	0.019	0.025	2.453	0.231
0.047	0.034	0.024	2.386	0.222	0.042	0.000	0.025	2.974	0.186
0.339	0.000	0.146	2.414	1.361	0.045	0.006	0.025	2.785	0.199
0.264	0.127	0.130	2.454	1.194	0.040	0.000	0.025	3.047	0.179
0.244	0.000	0.108	2.462	0.989	0.043	0.033	0.024	2.572	0.210
0.208	0.063	0.106	2.589	0.921	0.039	0.021	0.024	2.843	0.188
0.139	0.000	0.060	2.433	0.559	0.046	0.026	0.024	2.508	0.214
0.097	0.006	0.045	2.526	0.403	0.044	0.022	0.024	2.613	0.205
0.098	0.007	0.044	2.444	0.404	0.042	0.019	0.023	2.675	0.195
0.093	0.026	0.044	2.456	0.401	0.044	0.016	0.023	2.596	0.199
0.094	0.024	0.044	2.441	0.403	0.045	0.030	0.023	2.408	0.211
0.089	0.028	0.043	2.491	0.388	0.042	0.014	0.021	2.570	0.188
0.081	0.026	0.041	2.545	0.359	0.041	0.010	0.021	2.647	0.181
0.095	0.000	0.038	2.302	0.377	0.033	0.024	0.020	2.796	0.163
0.079	0.041	0.037	2.344	0.356	0.531	0.042	0.240	2.467	2.190
0.067	0.007	0.028	2.336	0.274	0.427	0.029	0.191	2.453	1.755
0.058	0.015	0.026	2.404	0.247	0.238	0.031	0.112	2.512	0.999
Hornblende biotite gneiss (54/1)					0.197	0.082	0.094	2.426	0.873
0.081	0.016	0.040	2.596	0.348	0.188	0.076	0.093	2.490	0.841
0.064	0.054	0.038	2.668	0.322	0.199	0.009	0.092	2.512	0.819
0.069	0.042	0.036	2.536	0.323	0.187	0.034	0.088	2.485	0.793
0.067	0.010	0.035	2.710	0.292	0.155	0.105	0.082	2.502	0.734
0.067	0.007	0.034	2.675	0.287	0.169	0.032	0.081	2.528	0.723
0.065	0.042	0.034	2.488	0.304	0.154	0.052	0.079	2.595	0.685
0.055	0.042	0.034	2.729	0.274	0.168	0.010	0.073	2.404	0.683
0.070	0.007	0.033	2.533	0.294	0.155	0.015	0.068	2.411	0.638
0.048	0.020	0.032	3.024	0.233	0.144	0.021	0.067	2.483	0.604
					0.128	0.053	0.065	2.532	0.574
					0.123	0.013	0.060	2.577	0.519
					0.104	0.000	0.044	2.391	0.415
					0.092	0.000	0.042	2.524	0.376
					0.068	0.044	0.034	2.444	0.317

Table A-2. EPMA analyses of zircons from garnet-bearing and garnet-free charnockites from the Madurai Block.

UO_2 (wt.%)	ThO_2 (wt.%)	PbO (wt.%)	Age (Ga)	ThO_2* (wt.%)	UO_2 (wt.%)	ThO_2 (wt.%)	PbO (wt.%)	Age (Ga)	ThO_2* (wt.%)
Charnockite (71/2)					*Charnockite (69/1) Contd.*				
0.142	0.204	0.094	2.660	0.793	0.136	0.112	0.029	1.144	0.586
0.206	0.046	0.026	0.830	0.747	0.146	0.118	0.028	1.033	0.623
0.205	0.059	0.026	0.814	0.755	0.114	0.083	0.024	1.178	0.481
0.167	0.000	0.026	1.050	0.577	0.107	0.034	0.021	1.209	0.410
Charnockite (69/1)					1.176	0.288	0.171	0.927	4.314
0.384	0.127	0.064	1.024	1.454	0.761	0.199	0.119	0.983	2.817
0.220	0.219	0.044	1.039	0.980	0.870	0.030	0.116	0.903	3.001
0.221	0.153	0.039	0.989	0.914	0.830	0.057	0.114	0.917	2.895
0.157	0.134	0.034	1.159	0.684	0.663	0.120	0.100	0.974	2.399
0.186	0.078	0.034	1.094	0.725	0.778	0.073	0.098	0.847	2.717
0.144	0.135	0.030	1.103	0.635	0.805	0.098	0.098	0.809	2.827
0.171	0.088	0.029	1.013	0.676					

Table A-2. *Contd.*

UO_2 (wt.%)	ThO_2 (wt.%)	PbO (wt.%)	Age (Ga)	ThO_2* (wt.%)
Charnockite (69/1) Contd.				
0.447	0.042	0.062	0.918	1.570
0.415	0.013	0.055	0.893	1.430
0.331	0.072	0.047	0.911	1.205
0.325	0.015	0.042	0.877	1.123
0.304	0.065	0.041	0.872	1.099
0.305	0.087	0.039	0.808	1.121
0.288	0.015	0.037	0.880	0.996
0.228	0.118	0.037	0.968	0.901
0.282	0.014	0.034	0.828	0.970
0.213	0.076	0.032	0.917	0.805
0.215	0.030	0.031	0.941	0.767
0.164	0.169	0.029	0.925	0.730
0.203	0.065	0.028	0.865	0.756
Charnockite (62/3)				
0.529	0.684	0.087	0.824	2.480
0.769	0.407	0.105	0.815	3.015
2.345	0.405	0.280	0.788	8.336
0.727	0.370	0.093	0.775	2.827
0.817	0.365	0.112	0.838	3.138
0.386	0.354	0.058	0.814	1.662
0.441	0.305	0.063	0.823	1.803
0.829	0.302	0.106	0.803	3.109
0.570	0.242	0.077	0.826	2.176
0.498	0.225	0.066	0.814	1.912
0.415	0.225	0.060	0.856	1.636
1.333	0.211	0.164	0.815	4.730
0.962	0.206	0.120	0.809	3.466
0.346	0.200	0.047	0.798	1.371
0.925	0.192	0.113	0.799	3.324
0.568	0.162	0.075	0.838	2.092
0.701	0.074	0.084	0.807	2.449
0.351	0.022	0.040	0.785	1.208
0.218	0.079	0.030	0.859	0.822
0.104	0.088	0.020	1.044	0.448
Charnockite (66/3)				
1.474	0.440	0.127	0.563	5.336
0.111	0.009	0.052	2.526	0.461
0.435	0.000	0.036	0.585	1.448
0.413	0.009	0.035	0.594	1.385
0.428	0.011	0.034	0.554	1.430
0.350	0.012	0.033	0.664	1.184
0.385	0.000	0.033	0.611	1.285
0.416	0.000	0.033	0.562	1.383
0.265	0.000	0.032	0.826	0.900
0.343	0.000	0.031	0.646	1.146
0.374	0.007	0.031	0.582	1.251
0.302	0.012	0.029	0.668	1.024
0.312	0.000	0.029	0.652	1.043
0.319	0.000	0.027	0.603	1.063
0.281	0.008	0.026	0.656	0.947
0.283	0.010	0.026	0.636	0.954
0.350	0.000	0.026	0.520	1.159
0.280	0.025	0.023	0.556	0.955
0.282	0.000	0.021	0.540	0.934
Charnockite (66/3) Contd.				
0.184	0.015	0.021	0.764	0.637
0.192	0.024	0.037	1.223	0.700
0.103	0.036	0.029	1.632	0.413
0.146	0.090	0.049	1.765	0.631
0.120	0.054	0.044	1.961	0.511
0.121	0.056	0.035	1.614	0.499
0.122	0.059	0.040	1.771	0.513
Charnockite (28/1)				
0.318	0.019	0.047	0.982	1.112
0.177	0.000	0.030	1.120	0.617
0.374	0.023	0.050	0.899	1.299
0.250	0.028	0.036	0.951	0.886
0.153	0.062	0.027	1.048	0.592
0.209	0.011	0.033	1.058	0.735
0.186	0.000	0.027	0.990	0.642
0.198	0.008	0.029	0.986	0.688
0.119	0.041	0.026	1.298	0.464
0.137	0.011	0.026	1.213	0.491
0.129	0.052	0.022	1.051	0.497
0.142	0.000	0.021	1.021	0.490
0.125	0.036	0.021	1.061	0.468
0.159	0.000	0.021	0.903	0.541
0.123	0.010	0.020	1.052	0.436
0.656	0.064	0.071	0.736	2.272
0.765	0.064	0.068	0.614	2.613
0.334	0.013	0.037	0.765	1.142
0.289	0.007	0.037	0.868	0.991
0.184	0.083	0.026	0.866	0.710
0.249	0.000	0.026	0.725	0.837
0.222	0.007	0.023	0.713	0.752
Charnockite (20/1)				
0.065	0.028	0.015	1.32	0.258
0.080	0.040	0.014	1.01	0.316
0.081	0.041	0.013	0.98	0.320
Garnet charnockite (60/2)				
0.254	0.009	0.024	0.667	0.859
0.242	0.012	0.024	0.691	0.825
Garnet charnockite (11/2)				
0.072	0.014	0.031	2.302	0.300
0.062	0.027	0.029	2.398	0.274
0.056	0.033	0.026	2.280	0.256
Garnet charnockite (36/4)				
0.303	0.000	0.021	0.505	1.000
0.227	0.000	0.020	0.625	0.757
0.171	0.008	0.027	1.033	0.598
Garnet charnockite (32/6)				
0.160	0.090	0.027	0.987	0.641
0.252	0.024	0.026	0.696	0.871
0.124	0.172	0.027	1.037	0.599
0.137	0.122	0.026	1.032	0.595
0.129	0.010	0.025	1.229	0.465
0.229	0.293	0.044	0.954	1.080

Table A-2. *Contd.*

UO_2 (wt.%)	ThO_2 (wt.%)	PbO (wt.%)	Age (Ga)	ThO_2* (wt.%)	UO_2 (wt.%)	ThO_2 (wt.%)	PbO (wt.%)	Age (Ga)	ThO_2* (wt.%)
Garnet charnockite (32/6) Contd.					*Garnet charnockite (32/6) Contd.*				
0.141	0.208	0.035	1.154	0.699	0.135	0.009	0.026	1.235	0.482
0.139	0.167	0.027	0.983	0.646	0.166	0.156	0.025	0.828	0.720
0.129	0.097	0.026	1.107	0.545	0.100	0.072	0.022	1.194	0.424
0.144	0.062	0.026	1.073	0.561	0.099	0.053	0.020	1.188	0.398
0.133	0.141	0.026	1.003	0.601	0.162	0.000	0.020	0.840	0.549

Table A-3. EPMA analyses of zircons from garnet-biotite gneiss, biotite gneiss, calc-silicate and pink metagranite from the Madurai Block.

UO_2 (wt.%)	ThO_2 (wt.%)	PbO (wt.%)	Age (Ga)	ThO_2* (wt.%)	UO_2 (wt.%)	ThO_2 (wt.%)	PbO (wt.%)	Age (Ga)	ThO_2* (wt.%)
Biotite gneiss (64/1)					*Biotite gneiss (64/1) Contd.*				
0.237	0.225	0.083	1.728	1.100	0.779	0.629	0.112	0.802	3.267
0.184	0.183	0.072	1.872	0.876	0.215	0.000	0.019	0.612	0.718
0.217	0.115	0.066	1.673	0.911	*Garnet biotite gneiss (32/7)*				
0.229	0.065	0.064	1.623	0.902	0.173	0.113	0.021	0.715	0.695
0.192	0.109	0.057	1.607	0.809	0.197	0.000	0.017	0.61	0.657
0.154	0.104	0.054	1.807	0.677	0.183	0.009	0.018	0.68	0.622
0.134	0.070	0.051	2.014	0.580	0.165	0.010	0.017	0.71	0.564
0.157	0.081	0.051	1.748	0.663	0.154	0.000	0.015	0.68	0.516
0.119	0.065	0.044	1.946	0.516	*Garnet biotite gneiss (67/1)*				
0.134	0.012	0.037	1.687	0.507	0.137	0.011	0.035	1.570	0.508
0.106	0.048	0.037	1.878	0.446	0.080	0.000	0.020	1.553	0.290
0.086	0.052	0.035	2.054	0.383	0.122	0.000	0.020	1.085	0.424
0.066	0.009	0.023	2.032	0.262	0.170	0.033	0.024	0.924	0.616
0.061	0.059	0.023	1.838	0.288	0.162	0.030	0.022	0.883	0.583
0.059	0.039	0.022	1.928	0.264	0.120	0.008	0.021	1.161	0.428
0.312	0.222	0.047	0.849	1.284	*Garnet biotite gneiss (32/5)*				
0.278	0.166	0.043	0.903	1.116	0.140	0.010	0.018	0.85	0.485
0.232	0.110	0.036	0.939	0.906	0.140	0.000	0.017	0.82	0.474
0.278	0.000	0.035	0.871	0.946	0.133	0.000	0.016	0.82	0.450
0.247	0.132	0.034	0.826	0.972	0.111	0.007	0.014	0.84	0.383
0.209	0.000	0.031	0.990	0.720	0.086	0.000	0.014	1.07	0.298
0.230	0.000	0.027	0.813	0.780	*Garnet biotite gneiss (30/1)*				
0.218	0.019	0.023	0.714	0.753	0.090	0.050	0.017	1.08	0.363
0.477	0.218	0.060	0.773	1.830	0.103	0.000	0.014	0.93	0.351
0.443	0.019	0.054	0.824	1.522	0.078	0.000	0.014	1.18	0.272
0.295	0.196	0.050	0.961	1.209	0.065	0.031	0.014	1.23	0.259
0.433	0.030	0.050	0.779	1.492	0.074	0.075	0.013	0.95	0.330
0.287	0.186	0.049	0.974	1.172	0.084	0.076	0.012	0.80	0.359
0.362	0.025	0.041	0.770	1.248	0.076	0.000	0.012	1.08	0.262
0.317	0.164	0.041	0.776	1.237	*Garnet biotite gneiss (71/1)*				
0.200	0.000	0.029	0.997	0.689	0.149	0.111	0.025	0.939	0.623
0.196	0.000	0.028	0.983	0.673	0.169	0.010	0.022	0.881	0.585
0.200	0.000	0.026	0.906	0.683	*Pink metagranite (16A/1)*				
0.178	0.000	0.023	0.894	0.608	0.801	0.185	0.070	0.580	2.848
0.462	0.010	0.037	0.572	1.545	0.720	0.063	0.059	0.570	2.456
0.296	0.008	0.025	0.585	0.993	0.344	0.231	0.035	0.592	1.377
0.279	0.017	0.024	0.608	0.948	0.354	0.201	0.033	0.558	1.376
0.319	0.000	0.024	0.538	1.058					

Table A-3. *Contd.*

UO_2 (wt.%)	ThO_2 (wt.%)	PbO (wt.%)	Age (Ga)	ThO_2* (wt.%)	UO_2 (wt.%)	ThO_2 (wt.%)	PbO (wt.%)	Age (Ga)	ThO_2* (wt.%)
Pink metagranite (16A/1) Contd.					*Pink metagranite (29/1) Contd.*				
0.310	0.213	0.031	0.578	1.245	0.190	0.000	0.023	0.832	0.644
0.254	0.261	0.029	0.609	1.106	0.202	0.007	0.021	0.715	0.686
0.256	0.157	0.025	0.578	1.010	0.170	0.000	0.020	0.819	0.576
0.329	0.219	0.040	0.703	1.324	0.188	0.000	0.020	0.729	0.631
0.243	0.147	0.025	0.623	0.958	*Calc-silicate (61/1)*				
0.243	0.107	0.024	0.623	0.917	0.094	0.022	0.015	1.00	0.346
0.215	0.151	0.024	0.652	0.870	0.078	0.000	0.015	1.24	0.273
0.259	0.000	0.024	0.654	0.866	0.071	0.000	0.014	1.26	0.252
Pink metagranite (29/1)					0.089	0.007	0.013	0.96	0.312
0.200	0.000	0.026	0.903	0.683	0.082	0.015	0.012	0.94	0.295

Table A-4. EPMA analyses of monazites from charnockites of the Madurai Block.

UO_2 (wt.%)	ThO_2 (wt.%)	PbO (wt.%)	Age (Ga)	ThO_2* (wt.%)	UO_2 (wt.%)	ThO_2 (wt.%)	PbO (wt.%)	Age (Ga)	ThO_2* (wt.%)
Garnet charnockite (11/2)					*Garnet charnockite (36/4) Contd.*				
0.142	8.583	0.217	0.566	9.053	0.278	4.748	0.125	0.521	5.668
0.392	2.223	0.085	0.566	3.527	0.093	4.126	0.104	0.553	4.435
0.429	2.476	0.092	0.555	3.901	0.103	4.029	0.093	0.503	4.368
0.175	8.650	0.217	0.555	9.230	0.234	3.485	0.096	0.533	4.262
0.151	8.602	0.213	0.553	9.104	0.244	3.233	0.086	0.501	4.040
0.365	2.330	0.083	0.553	3.540	0.083	3.583	0.086	0.524	3.856
0.177	8.146	0.203	0.547	8.732	0.101	3.427	0.083	0.519	3.762
0.189	3.340	0.092	0.546	3.965	*Garnet charnockite (60/2)*				
0.350	2.252	0.078	0.540	3.413	0.300	2.757	0.090	0.568	3.754
0.173	8.631	0.210	0.538	9.204	0.383	5.971	0.174	0.565	7.245
0.209	3.204	0.087	0.527	3.895	0.366	5.272	0.153	0.557	6.486
0.201	9.126	0.219	0.527	9.792	0.331	4.379	0.128	0.552	5.477
0.328	2.971	0.090	0.521	4.058	0.322	4.126	0.120	0.546	5.194
0.318	3.301	0.095	0.515	4.354	0.293	3.981	0.114	0.545	4.953
0.227	2.767	0.077	0.514	3.517	0.367	5.408	0.152	0.542	6.626
0.197	3.223	0.084	0.512	3.876	0.302	4.136	0.117	0.539	5.136
0.235	6.214	0.151	0.511	6.989	0.340	5.039	0.141	0.538	6.167
0.204	5.961	0.143	0.510	6.635	0.271	3.078	0.090	0.537	3.975
0.194	4.942	0.117	0.496	5.582	0.395	6.505	0.177	0.534	7.813
Garnet charnockite (36/4)					0.301	3.699	0.106	0.531	4.696
0.229	9.612	0.248	0.563	10.373	0.366	7.049	0.186	0.530	8.262
0.218	9.495	0.246	0.567	10.220	0.375	5.320	0.147	0.529	6.562
0.223	9.466	0.237	0.548	10.204	0.379	5.835	0.158	0.525	7.089
0.213	9.388	0.237	0.553	10.094	0.371	5.330	0.145	0.522	6.557
0.236	8.874	0.219	0.534	9.656	0.327	4.330	0.118	0.517	5.411
0.226	8.903	0.223	0.544	9.651	0.355	5.524	0.146	0.516	6.698
0.217	6.466	0.157	0.515	7.182	0.368	5.854	0.154	0.513	7.073
0.732	4.612	0.159	0.533	7.038	0.358	5.699	0.150	0.513	6.883
0.238	5.913	0.148	0.521	6.702	0.365	5.757	0.151	0.512	6.964
0.210	5.893	0.144	0.517	6.587	0.363	5.650	0.145	0.500	6.849
0.088	6.165	0.148	0.540	6.458	*Charnockite (66/3)*				
0.142	5.961	0.143	0.524	6.430	0.219	17.738	0.406	0.519	18.463
0.229	5.592	0.148	0.551	6.350	0.253	19.311	0.457	0.535	20.149
0.220	5.505	0.141	0.535	6.234	0.941	9.854	0.290	0.528	12.972
0.376	4.961	0.134	0.512	6.204	0.262	16.039	0.376	0.525	16.908
0.243	5.359	0.145	0.556	6.167	0.323	14.398	0.337	0.514	15.465
0.411	4.757	0.137	0.527	6.118	0.633	13.117	0.358	0.555	15.218
0.451	4.408	0.132	0.529	5.903	1.233	15.466	0.470	0.566	19.560
0.103	5.485	0.124	0.501	5.827					

Table A-4. *Contd.*

UO_2 (wt.%)	ThO_2 (wt.%)	PbO (wt.%)	Age (Ga)	ThO_2* (wt.%)	UO_2 (wt.%)	ThO_2 (wt.%)	PbO (wt.%)	Age (Ga)	ThO_2* (wt.%)
Charnockite (66/3) Contd.					*Charnockite (66/3) Contd.*				
0.228	16.893	0.382	0.510	17.646	0.393	1.553	0.059	0.487	2.851
0.329	14.010	0.336	0.525	15.099	*Charnockite (71/2)*				
0.510	10.835	0.280	0.529	12.523	0.420	26.019	0.633	0.544	27.411
0.489	10.767	0.266	0.507	12.383	0.406	25.534	0.610	0.535	26.881
0.485	10.631	0.272	0.525	12.237	0.375	24.670	0.596	0.542	25.914
0.520	10.485	0.266	0.515	12.207	0.215	14.990	0.356	0.534	15.703
0.528	10.194	0.265	0.523	11.942	0.205	13.641	0.319	0.525	14.319
0.441	10.417	0.268	0.532	11.879	0.169	13.243	0.310	0.530	13.803
0.414	10.427	0.262	0.524	11.798	0.146	11.660	0.268	0.521	12.145
0.578	9.845	0.255	0.512	11.758	0.168	11.485	0.270	0.529	12.043
0.431	10.291	0.265	0.533	11.720	0.146	10.699	0.248	0.523	11.182
0.484	5.165	0.143	0.500	6.766	0.141	10.553	0.244	0.522	11.021
0.474	3.748	0.119	0.528	5.318	0.124	8.883	0.210	0.533	9.294
0.444	3.427	0.112	0.539	4.900	0.110	7.592	0.166	0.493	7.954
0.353	3.583	0.099	0.494	4.747	0.144	7.350	0.177	0.534	7.828
0.470	2.961	0.100	0.521	4.516	0.107	7.398	0.162	0.495	7.750
0.456	2.854	0.090	0.488	4.361	0.097	6.990	0.157	0.508	7.312
0.476	2.777	0.096	0.522	4.351	0.122	6.738	0.153	0.506	7.142
0.452	2.748	0.100	0.556	4.248	0.137	6.553	0.163	0.548	7.008
0.454	2.175	0.081	0.518	3.678	0.131	5.893	0.138	0.515	6.326
0.422	2.223	0.074	0.482	3.617	0.130	5.631	0.125	0.488	6.060
0.361	2.350	0.085	0.563	3.550	0.102	5.699	0.126	0.494	6.035
0.232	2.117	0.064	0.525	2.885	0.116	5.534	0.129	0.516	5.919

Table A-5. EPMA analyses of monazites from garnet-biotite gneiss and pink metagranite.

UO_2 (wt.%)	ThO_2 (wt.%)	PbO (wt.%)	Age (Ga)	ThO_2* (wt.%)	UO_2 (wt.%)	ThO_2 (wt.%)	PbO (wt.%)	Age (Ga)	ThO_2* (wt.%)
Garnet biotite gneiss (32/7)					*Garnet biotite gneiss (67/1)*				
0.831	21.806	0.566	0.544	24.562	1.152	8.631	0.273	0.517	12.443
0.844	21.010	0.537	0.532	23.805	1.393	11.049	0.329	0.496	15.651
0.554	17.369	0.436	0.536	19.205	1.168	8.893	0.290	0.536	12.763
0.408	15.485	0.380	0.533	16.838	1.637	12.699	0.422	0.548	18.129
0.418	15.311	0.391	0.552	16.698	1.939	18.204	0.522	0.501	24.611
0.783	21.495	0.539	0.528	24.089	1.237	11.466	0.351	0.533	15.563
0.668	14.233	0.366	0.526	16.446	1.205	10.932	0.332	0.525	14.922
0.625	14.456	0.377	0.538	16.527	1.239	13.184	0.379	0.518	17.285
0.593	20.631	0.507	0.529	22.595	1.279	13.806	0.397	0.519	18.039
0.625	23.796	0.573	0.523	25.866	1.198	13.864	0.417	0.551	17.840
0.271	16.602	0.398	0.537	17.501	1.285	15.301	0.460	0.554	19.566
0.282	15.913	0.398	0.557	16.850	1.219	10.699	0.331	0.530	14.736
0.284	16.233	0.392	0.538	17.175	1.249	10.670	0.319	0.509	14.801
0.190	9.709	0.242	0.552	10.338	1.214	11.000	0.343	0.538	15.024
0.503	9.816	0.261	0.536	11.482	1.489	11.282	0.368	0.536	16.218
0.295	9.670	0.239	0.530	10.648	1.498	11.359	0.367	0.531	16.322
0.651	8.165	0.230	0.526	10.322	0.609	12.583	0.373	0.601	14.610
0.652	7.903	0.219	0.513	10.058	1.069	10.068	0.318	0.551	13.614
0.638	7.893	0.233	0.550	10.009	1.116	10.272	0.320	0.541	13.970
0.657	7.447	0.211	0.519	9.620	0.555	8.806	0.258	0.571	10.650
0.660	6.786	0.203	0.534	8.975	0.461	7.408	0.224	0.591	8.944
0.658	5.155	0.168	0.541	7.335	0.491	8.126	0.249	0.601	9.762
0.668	4.913	0.164	0.544	7.129	1.345	14.058	0.411	0.524	18.511
0.588	5.126	0.156	0.522	7.073	1.303	13.583	0.404	0.532	17.898
0.592	5.184	0.163	0.540	7.147	*Garnet biotite gneiss (71/1)*				
0.734	1.104	0.074	0.492	3.529	0.131	7.845	0.189	0.537	8.280

Table A-5. *Contd.*

UO_2 (wt.%)	ThO_2 (wt.%)	PbO (wt.%)	Age (Ga)	ThO_2* (wt.%)	UO_2 (wt.%)	ThO_2 (wt.%)	PbO (wt.%)	Age (Ga)	ThO_2* (wt.%)
Garnet biotite gneiss (71/1) Contd.					*Garnet biotite gneiss (30/1) Contd.*				
0.092	7.553	0.180	0.541	7.859	0.145	13.942	0.310	0.508	14.421
0.182	8.845	0.206	0.516	9.448	0.113	8.456	0.206	0.551	8.830
0.163	8.165	0.200	0.541	8.707	0.217	3.913	0.112	0.572	4.635
0.126	6.874	0.162	0.526	7.291	0.226	3.942	0.106	0.532	4.690
0.108	6.223	0.150	0.537	6.583	0.217	4.049	0.106	0.524	4.768
0.123	8.165	0.189	0.519	8.573	*Pink metagranite (16A/1)*				
0.102	7.951	0.182	0.518	8.288	0.165	9.447	0.238	0.561	9.994
0.101	6.874	0.161	0.526	7.208	0.304	8.155	0.222	0.570	9.164
0.101	6.573	0.156	0.533	6.907	0.335	10.689	0.285	0.568	11.802
0.096	6.553	0.158	0.542	6.872	0.334	10.816	0.289	0.571	11.925
0.116	6.728	0.155	0.513	7.113	0.165	12.592	0.307	0.552	13.138
Garnet biotite gneiss (30/1)					0.273	14.505	0.376	0.575	15.412
0.175	3.563	0.082	0.470	4.140	0.292	8.117	0.211	0.547	9.085
0.167	3.757	0.092	0.504	4.309	0.373	12.029	0.315	0.560	13.266
0.152	4.718	0.116	0.527	5.220	0.385	12.107	0.309	0.545	13.385
0.128	5.068	0.125	0.537	5.492	0.494	11.563	0.313	0.559	13.203
0.102	4.990	0.121	0.535	5.329	0.296	7.427	0.194	0.543	8.409
0.124	6.214	0.146	0.519	6.623	0.272	8.864	0.229	0.552	9.767
0.175	7.301	0.182	0.544	7.882	0.275	6.913	0.182	0.547	7.826
0.115	7.854	0.175	0.501	8.235	0.299	6.932	0.179	0.535	7.923
0.105	5.398	0.128	0.524	5.744	0.398	11.680	0.310	0.562	13.002
0.423	4.039	0.121	0.526	5.441	0.210	11.447	0.292	0.567	12.144
0.357	4.291	0.122	0.525	5.474	0.241	9.738	0.235	0.526	10.537
0.118	4.359	0.108	0.534	4.751	0.188	12.505	0.300	0.538	13.128
0.120	7.010	0.147	0.470	7.405	0.188	8.350	0.204	0.536	8.974
0.111	7.107	0.167	0.527	7.475	0.239	9.893	0.229	0.505	10.682
0.163	5.825	0.132	0.490	6.363	0.202	13.621	0.338	0.557	14.292
0.133	4.573	0.102	0.480	5.011	0.480	10.631	0.285	0.551	12.223
0.148	5.718	0.125	0.474	6.205	0.523	10.398	0.287	0.558	12.133
0.151	5.816	0.137	0.514	6.315	0.314	17.544	0.442	0.561	18.587
0.112	5.175	0.111	0.472	5.545	0.306	13.175	0.329	0.546	14.190
0.092	5.534	0.122	0.494	5.839					

Table A-6. EPMA analyses of uraninite and huttonite from the Madurai Block.

UO_2 (wt.%)	ThO_2 (wt.%)	PbO (wt.%)	Age (Ga)	ThO_2* (wt.%)	UO_2 (wt.%)	ThO_2 (wt.%)	PbO (wt.%)	Age (Ga)	ThO_2* (wt.%)
Uraninite (Pinkgranite 29/1)					*Uraninite (Pinkgranite 29/1) Contd.*				
81.10	8.52	6.12	0.521	276.96	83.76	5.32	5.93	0.496	282.05
83.83	5.97	6.26	0.521	283.46	83.14	6.53	5.90	0.495	281.18
78.49	6.78	5.87	0.520	266.56	84.14	5.42	5.94	0.495	283.36
80.70	7.04	6.03	0.519	274.13	85.31	5.26	6.01	0.494	287.03
84.86	3.92	6.26	0.519	284.75	83.95	5.35	5.91	0.494	282.65
83.17	5.94	6.15	0.516	281.14	83.17	5.26	5.83	0.492	279.91
83.99	5.68	6.17	0.514	283.52	84.19	5.20	5.90	0.492	283.23
85.23	4.27	6.23	0.514	286.23	84.52	5.53	5.91	0.491	284.63
81.62	5.43	5.94	0.509	275.35	81.26	7.28	5.71	0.489	275.58
84.95	5.13	6.15	0.508	286.02	83.70	5.36	5.80	0.487	281.68
79.85	8.08	5.81	0.504	272.04	*Uraninite (Biotite gneiss 64/1)*				
78.88	8.42	5.74	0.503	269.15	78.42	5.60	5.87	0.523	265.20
79.35	7.92	5.76	0.503	270.19	79.56	5.31	5.96	0.524	268.72
83.83	5.42	6.01	0.502	282.49	78.22	5.16	5.69	0.509	263.83
80.93	7.56	5.85	0.502	275.05	76.52	6.12	5.96	0.541	259.80
80.85	7.34	5.83	0.501	274.53	79.24	5.55	5.88	0.519	267.79
83.62	5.35	5.98	0.501	281.71	83.27	3.47	5.98	0.507	278.77
83.67	5.46	5.97	0.500	281.95	79.28	4.74	5.80	0.513	267.01
77.07	9.68	5.57	0.498	264.30	77.56	6.20	5.81	0.521	262.93

Table A-6. *Contd.*

UO_2 (wt.%)	ThO_2 (wt.%)	PbO (wt.%)	Age (Ga)	ThO_2* (wt.%)	UO_2 (wt.%)	ThO_2 (wt.%)	PbO (wt.%)	Age (Ga)	ThO_2* (wt.%)
Uraninite (Biotite gneiss 64/1) Contd.					*Uraninite (Garnet biotite gneiss 67/1) Contd.*				
78.26	5.92	5.92	0.527	265.10	83.41	6.97	6.46	0.538	283.44
79.38	4.23	5.91	0.522	267.02	83.41	7.19	6.33	0.527	283.42
79.72	4.40	6.03	0.530	268.47	83.47	7.29	6.20	0.517	283.48
80.21	4.78	6.24	0.544	270.76	82.71	7.76	6.39	0.535	281.84
80.21	4.78	6.24	0.544	270.76	84.74	6.90	6.22	0.512	287.17
80.73	4.23	5.97	0.519	271.42	82.82	8.02	6.27	0.525	282.22
75.93	6.77	5.65	0.517	258.02	82.88	7.43	6.17	0.517	281.67
82.49	3.68	6.05	0.516	276.64	85.38	5.31	6.22	0.511	287.71
77.84	5.33	6.02	0.540	263.37	87.00	3.70	6.33	0.512	291.49
75.76	5.70	5.58	0.514	256.33	84.09	7.20	6.37	0.527	285.66
81.23	4.41	6.25	0.539	273.66	84.04	7.04	6.24	0.517	285.14
Uraninite (Charnockite 66/3)					84.40	7.40	6.23	0.513	286.59
83.45	3.50	5.35	0.455	278.29	84.32	7.68	6.11	0.504	286.41
84.96	3.73	5.56	0.463	283.68	84.55	7.35	5.86	0.484	286.39
84.74	3.93	5.78	0.481	283.55	84.66	7.32	6.11	0.503	287.14
84.28	4.04	5.83	0.488	282.28	83.75	8.19	5.92	0.491	284.77
83.48	4.37	5.92	0.499	280.21	83.44	8.10	5.97	0.497	283.78
83.65	4.47	5.84	0.491	280.71	83.73	7.67	6.03	0.501	284.39
83.91	4.42	5.95	0.499	281.68	82.36	6.84	8.68	0.719	283.81
84.36	3.95	6.15	0.513	283.00	84.12	7.08	5.80	0.482	284.67
83.95	3.89	5.60	0.471	280.68	84.53	6.82	5.87	0.485	285.83
85.38	3.89	5.71	0.473	285.43	82.90	7.43	5.57	0.469	280.71
85.21	3.81	5.94	0.492	285.22	83.30	6.24	6.07	0.509	281.70
84.80	4.21	5.91	0.491	284.25	84.15	6.64	6.04	0.501	284.74
84.37	4.57	5.90	0.492	283.19	83.79	6.95	6.36	0.528	284.46
83.87	4.43	6.05	0.507	281.74	83.43	7.50	6.09	0.508	283.35
86.62	3.53	6.13	0.500	289.75	84.69	7.35	5.99	0.493	287.06
86.57	3.52	6.16	0.502	289.64	84.54	6.95	6.28	0.517	286.72
85.67	4.08	6.16	0.506	287.31	85.04	7.10	6.12	0.502	288.17
84.52	4.43	5.96	0.496	283.65	85.67	6.57	6.22	0.507	289.83
84.77	4.47	5.94	0.493	284.45	82.12	8.17	6.05	0.510	279.77
84.69	4.24	6.21	0.515	284.45	85.62	7.14	6.21	0.506	290.20
Uraninite (Garnet biotite gneiss 67/1)					85.12	6.87	6.29	0.515	288.47
82.46	6.85	5.83	0.493	279.19	83.81	6.98	5.89	0.491	283.75
82.66	6.92	5.88	0.496	279.98	85.82	5.59	6.22	0.508	289.36
82.54	6.92	6.33	0.533	280.37	85.05	7.36	6.29	0.515	288.73
83.28	7.00	6.28	0.525	282.75	82.48	6.73	9.53	0.783	285.59
84.50	7.04	6.30	0.519	286.70	85.04	6.97	6.37	0.522	288.48
84.34	6.94	6.15	0.508	285.81	84.40	7.21	6.37	0.525	286.66
84.94	6.59	6.17	0.507	287.44	84.17	7.33	6.62	0.545	286.46
84.62	7.10	6.26	0.515	287.07	83.57	7.40	6.63	0.550	284.63
83.99	7.13	6.13	0.508	284.87	83.19	7.16	6.79	0.565	283.48
80.97	6.75	8.84	0.742	279.58	84.83	5.65	6.11	0.505	286.07
83.63	7.03	6.10	0.508	283.58	83.78	4.81	6.46	0.539	282.53
83.34	7.80	6.22	0.518	283.59	*Huttonite (Biotite gneiss 64/1)*				
83.84	7.47	6.15	0.510	284.73	27.45	45.00	3.07	0.534	135.95
84.30	6.92	5.62	0.467	284.76	27.69	44.28	3.00	0.522	135.95
84.82	6.93	6.04	0.497	287.14	27.15	44.78	3.00	0.526	134.70
85.96	5.49	6.33	0.516	289.91	26.85	45.13	2.90	0.512	133.93
84.46	6.32	6.81	0.560	286.74	28.16	43.10	3.16	0.547	136.51
84.94	6.76	6.52	0.534	288.19	27.62	44.26	3.00	0.523	135.70
83.96	6.83	6.33	0.525	284.81					

Table A-7. EPMA analyses of zircons from the Trivandrum Block.

UO_2 (wt.%)	ThO_2 (wt.%)	PbO (wt.%)	Age (Ga)	ThO_2* (wt.%)	UO_2 (wt.%)	ThO_2 (wt.%)	PbO (wt.%)	Age (Ga)	ThO_2* (wt.%)
Garnet biotite gneiss (5b)					*Garnet biotite gneiss (5b) Contd.*				
1.392	0.113	0.415	1.790	5.293	0.134	0.076	0.033	1.392	0.554
1.205	0.083	0.283	1.473	4.420	0.157	0.035	0.031	1.222	0.587
0.880	0.076	0.238	1.651	3.302	0.070	0.021	0.030	2.297	0.299
0.829	0.056	0.232	1.711	3.114	0.125	0.066	0.027	1.225	0.507
0.711	0.302	0.222	1.731	2.931	0.120	0.000	0.026	1.379	0.428
0.595	0.147	0.190	1.833	2.371	0.109	0.075	0.025	1.282	0.461
0.701	0.000	0.162	1.481	2.526	0.320	0.016	0.025	0.551	1.079
0.564	0.033	0.158	1.711	2.116	0.056	0.012	0.025	2.368	0.234
0.569	0.000	0.137	1.533	2.062	0.100	0.019	0.024	1.440	0.379
0.707	0.036	0.119	1.111	2.495	0.336	0.000	0.023	0.496	1.108
0.549	0.007	0.114	1.342	1.957	0.159	0.000	0.021	0.901	0.542
0.515	0.015	0.112	1.396	1.856	0.246	0.013	0.021	0.589	0.833
0.341	0.038	0.106	1.845	1.316	0.089	0.012	0.020	1.428	0.330
0.531	0.019	0.103	1.265	1.894	0.757	0.025	0.109	0.968	2.627
0.596	0.012	0.102	1.135	2.089	0.309	0.009	0.033	0.740	1.049
0.709	0.033	0.101	0.958	2.466	0.323	0.000	0.031	0.678	1.082
0.469	0.011	0.097	1.334	1.678	0.297	0.008	0.030	0.706	1.005
0.471	0.018	0.097	1.322	1.690	0.343	0.015	0.030	0.604	1.157
0.782	0.023	0.096	0.839	2.680	0.332	0.015	0.029	0.608	1.122
0.481	0.035	0.092	1.236	1.727	0.334	0.020	0.027	0.571	1.130
0.546	0.066	0.091	1.077	1.958	0.308	0.007	0.027	0.618	1.033
0.463	0.023	0.085	1.194	1.645	0.283	0.017	0.023	0.560	0.956
0.352	0.028	0.082	1.453	1.294	0.263	0.006	0.022	0.600	0.880
0.382	0.000	0.080	1.363	1.359	*Garnet biotite gneiss (7)*				
0.288	0.010	0.080	1.702	1.072	0.394	0.027	0.112	1.731	1.484
1.146	0.025	0.077	0.475	3.803	0.298	0.023	0.071	1.500	1.097
0.622	0.028	0.076	0.827	2.140	0.203	0.000	0.067	1.982	0.771
0.302	0.020	0.075	1.549	1.116	0.284	0.000	0.055	1.277	1.003
0.590	0.027	0.074	0.852	2.034	0.134	0.017	0.048	2.061	0.530
0.405	0.019	0.073	1.181	1.436	0.530	0.000	0.046	0.619	1.767
0.351	0.049	0.072	1.300	1.291	0.450	0.000	0.043	0.673	1.509
0.382	0.039	0.070	1.186	1.377	0.557	0.000	0.042	0.536	1.847
0.164	0.000	0.063	2.224	0.643	0.164	0.000	0.040	1.558	0.596
0.417	0.000	0.061	0.990	1.435	0.224	0.009	0.040	1.171	0.792
0.215	0.030	0.060	1.683	0.821	0.162	0.010	0.038	1.463	0.592
0.251	0.007	0.060	1.517	0.914	0.423	0.000	0.037	0.619	1.413
0.398	0.034	0.057	0.948	1.399	0.175	0.013	0.036	1.330	0.633
0.219	0.068	0.054	1.449	0.853	0.209	0.006	0.036	1.147	0.735
0.174	0.006	0.052	1.822	0.654	0.430	0.009	0.036	0.592	1.439
0.308	0.000	0.049	1.073	1.067	0.379	0.000	0.035	0.641	1.268
0.322	0.022	0.048	0.987	1.131	0.207	0.006	0.034	1.093	0.724
0.127	0.031	0.046	2.022	0.517	0.185	0.000	0.033	1.174	0.649
0.285	0.016	0.045	1.042	1.001	0.134	0.014	0.033	1.507	0.497
0.245	0.000	0.044	1.178	0.859	0.381	0.011	0.031	0.566	1.278
0.329	0.000	0.042	0.877	1.122	0.381	0.000	0.030	0.567	1.264
0.226	0.000	0.042	1.226	0.795	0.179	0.000	0.030	1.107	0.623
0.228	0.008	0.042	1.203	0.809	0.165	0.000	0.030	1.186	0.578
0.126	0.024	0.042	1.901	0.499	0.139	0.000	0.029	1.346	0.496
0.196	0.000	0.040	1.336	0.697	0.137	0.000	0.029	1.355	0.488
0.237	0.000	0.037	1.063	0.821	0.174	0.006	0.027	1.025	0.605
0.104	0.010	0.037	2.068	0.409	0.126	0.006	0.026	1.340	0.455
0.157	0.052	0.037	1.398	0.612	0.287	0.000	0.024	0.603	0.957
0.117	0.020	0.037	1.840	0.456	0.132	0.000	0.023	1.159	0.461
0.169	0.008	0.036	1.368	0.611	0.211	0.000	0.023	0.746	0.712
0.312	0.024	0.036	0.781	1.077	0.184	0.000	0.022	0.834	0.626
0.207	0.000	0.035	1.128	0.721	0.215	0.000	0.022	0.704	0.724
0.343	0.000	0.035	0.712	1.153	0.144	0.000	0.021	1.011	0.495
0.103	0.007	0.034	1.939	0.396	0.239	0.010	0.021	0.602	0.806

Table A-7. *Contd.*

UO_2 (wt.%)	ThO_2 (wt.%)	PbO (wt.%)	Age (Ga)	ThO_2* (wt.%)	UO_2 (wt.%)	ThO_2 (wt.%)	PbO (wt.%)	Age (Ga)	ThO_2* (wt.%)
Garnet biotite gneiss (7) Contd.					*Khondalite (8) Contd.*				
0.106	0.013	0.020	1.220	0.385	0.347	0.000	0.028	0.569	1.154
0.373	0.007	0.033	0.614	1.251	0.323	0.000	0.026	0.563	1.072
0.241	0.000	0.030	0.865	0.821	0.139	0.000	0.024	1.146	0.486
0.328	0.007	0.027	0.585	1.098	0.294	0.000	0.023	0.552	0.975
0.315	0.008	0.027	0.605	1.058	0.248	0.000	0.022	0.618	0.826
0.288	0.000	0.026	0.646	0.964	0.282	0.000	0.021	0.533	0.934
0.287	0.008	0.026	0.627	0.967	*Charnockite (5a)*				
0.284	0.000	0.025	0.627	0.948	0.514	0.019	0.071	0.929	1.779
0.310	0.000	0.025	0.577	1.030	0.799	0.038	0.069	0.599	2.699
0.290	0.007	0.024	0.591	0.974	0.560	0.027	0.055	0.676	1.904
0.270	0.000	0.024	0.616	0.901	0.194	0.054	0.055	1.639	0.765
0.281	0.009	0.023	0.586	0.943	0.572	0.030	0.051	0.616	1.937
0.296	0.009	0.023	0.555	0.990	0.526	0.021	0.048	0.634	1.778
0.265	0.000	0.022	0.594	0.882	0.516	0.021	0.045	0.605	1.742
0.227	0.000	0.021	0.656	0.760	0.468	0.030	0.044	0.646	1.594
0.216	0.009	0.021	0.659	0.733	0.432	0.014	0.042	0.671	1.460
0.185	0.007	0.020	0.760	0.632	0.470	0.022	0.042	0.617	1.590
Khondalite (8)					0.558	0.019	0.042	0.526	1.867
0.875	0.110	0.245	1.685	3.330	0.465	0.048	0.040	0.588	1.597
0.700	0.099	0.196	1.682	2.676	0.459	0.017	0.039	0.590	1.543
0.299	0.158	0.115	2.015	1.298	0.424	0.047	0.037	0.596	1.458
0.423	0.061	0.107	1.544	1.597	0.351	0.015	0.037	0.717	1.196
0.235	0.113	0.098	2.166	1.027	0.481	0.020	0.036	0.526	1.613
0.235	0.086	0.092	2.091	0.993	0.387	0.049	0.036	0.629	1.342
0.221	0.100	0.084	2.020	0.946	0.376	0.058	0.035	0.631	1.315
0.226	0.075	0.075	1.854	0.922	0.353	0.031	0.035	0.677	1.215
0.328	0.044	0.074	1.401	1.218	0.394	0.015	0.035	0.617	1.330
0.402	0.009	0.068	1.125	1.409	0.095	0.044	0.034	1.936	0.402
0.571	0.000	0.062	0.756	1.927	0.413	0.035	0.034	0.567	1.408
0.203	0.048	0.061	1.747	0.800	0.343	0.058	0.034	0.660	1.206
0.192	0.067	0.059	1.728	0.776	0.342	0.033	0.034	0.674	1.181
0.132	0.037	0.050	2.079	0.546	0.368	0.011	0.034	0.641	1.239
0.381	0.000	0.049	0.885	1.298	0.352	0.014	0.032	0.627	1.191
0.113	0.091	0.048	2.071	0.526	0.268	0.021	0.032	0.800	0.927
0.194	0.081	0.048	1.428	0.775	0.316	0.017	0.032	0.690	1.077
0.163	0.106	0.048	1.572	0.700	0.356	0.046	0.031	0.592	1.232
0.096	0.038	0.047	2.470	0.426	0.382	0.019	0.031	0.559	1.289
0.192	0.018	0.042	1.393	0.702	0.094	0.059	0.030	1.702	0.407
0.095	0.072	0.041	2.132	0.441	0.304	0.031	0.030	0.673	1.049
0.096	0.069	0.041	2.124	0.442	0.265	0.035	0.029	0.729	0.928
0.208	0.021	0.040	1.237	0.752	0.300	0.017	0.029	0.662	1.021
0.120	0.026	0.036	1.746	0.469	0.289	0.017	0.029	0.684	0.987
0.089	0.049	0.036	2.063	0.392	0.233	0.027	0.028	0.813	0.818
0.113	0.044	0.036	1.759	0.463	0.356	0.042	0.028	0.537	1.223
0.156	0.047	0.035	1.347	0.601	0.299	0.019	0.026	0.601	1.014
0.199	0.040	0.027	0.888	0.718	0.268	0.064	0.023	0.575	0.955
0.083	0.038	0.024	1.615	0.341	0.063	0.058	0.023	1.781	0.293
0.290	0.008	0.024	0.578	0.973	0.260	0.024	0.023	0.603	0.891
0.320	0.006	0.024	0.526	1.067	0.483	0.038	0.039	0.559	1.641
0.235	0.000	0.023	0.696	0.788	0.366	0.047	0.032	0.593	1.265
0.054	0.049	0.023	2.049	0.255	0.309	0.038	0.030	0.655	1.072
0.304	0.000	0.022	0.516	1.007	0.328	0.021	0.029	0.612	1.114
0.208	0.007	0.021	0.711	0.706	0.282	0.014	0.027	0.656	0.956
0.224	0.006	0.021	0.646	0.755	0.324	0.024	0.027	0.568	1.102
0.036	0.062	0.020	2.251	0.205	0.311	0.022	0.025	0.552	1.052
0.788	0.113	0.220	1.675	3.010	0.294	0.027	0.022	0.517	1.001

Table A-8. EPMA analyses of monazites from the Trivandrum Block.

UO_2 (wt.%)	ThO_2 (wt.%)	PbO (wt.%)	Age (Ga)	ThO_2* (wt.%)	UO_2 (wt.%)	ThO_2 (wt.%)	PbO (wt.%)	Age (Ga)	ThO_2* (wt.%)
Khondalite (8)					*Garnet biotite gneiss (5b) Contd.*				
0.269	7.820	0.200	0.543	8.712	0.268	7.890	0.206	0.555	8.779
1.243	4.200	0.205	0.580	8.333	1.261	16.210	0.482	0.557	20.395
0.268	8.230	0.205	0.531	9.119	1.339	18.840	0.551	0.558	23.284
0.569	7.220	0.217	0.561	9.111	0.747	10.380	0.305	0.560	12.860
0.263	8.650	0.221	0.548	9.521	1.349	14.460	0.450	0.561	18.938
0.772	6.830	0.222	0.558	9.392	1.049	16.930	0.488	0.563	20.414
0.561	7.510	0.225	0.566	9.373	0.845	12.810	0.375	0.566	15.617
1.622	4.280	0.239	0.581	9.673	1.500	5.630	0.255	0.567	10.613
0.732	7.820	0.245	0.563	10.251	0.723	6.630	0.217	0.568	9.032
1.520	5.030	0.248	0.579	10.083	0.750	10.040	0.302	0.569	12.533
0.499	8.860	0.249	0.557	10.517	0.600	9.090	0.268	0.570	11.082
0.546	9.020	0.249	0.542	10.829	0.772	10.880	0.326	0.571	13.445
0.260	10.340	0.249	0.525	11.199	0.478	11.140	0.310	0.574	12.728
1.491	4.920	0.251	0.597	9.886	0.759	5.690	0.200	0.575	8.213
0.579	8.590	0.251	0.562	10.511	0.823	13.420	0.396	0.578	16.157
0.293	9.900	0.252	0.546	10.870	1.018	5.160	0.210	0.579	8.546
0.638	8.410	0.253	0.565	10.531	0.784	12.730	0.378	0.581	15.339
0.651	8.570	0.255	0.559	10.731	0.532	10.260	0.302	0.591	12.030
0.654	8.410	0.259	0.578	10.586	0.340	6.220	0.252	0.802	7.373
1.492	5.480	0.269	0.606	10.453	0.368	8.290	0.328	0.806	9.538
0.562	9.660	0.269	0.551	11.526	0.270	8.960	0.376	0.890	9.880
1.517	5.810	0.270	0.587	10.858	0.258	8.770	0.377	0.913	9.651
0.905	8.340	0.275	0.571	11.346	0.426	8.560	0.394	0.920	10.017
1.585	6.580	0.296	0.588	11.853	0.318	15.820	0.717	0.989	16.914
0.341	11.930	0.297	0.536	13.060	0.253	10.390	0.478	0.991	11.260
0.330	11.800	0.297	0.544	12.895	0.391	8.350	0.412	0.992	9.697
1.660	6.850	0.301	0.573	12.369	0.274	12.230	0.561	0.993	13.174
0.420	12.290	0.305	0.526	13.682	0.270	11.490	0.542	1.017	12.422
0.314	12.200	0.307	0.547	13.241	0.282	13.940	0.655	1.023	14.913
1.973	6.080	0.309	0.576	12.638	0.393	9.270	0.478	1.048	10.628
1.639	6.960	0.312	0.593	12.415	0.258	12.620	0.620	1.068	13.514
1.619	6.940	0.314	0.600	12.333	0.396	8.220	0.449	1.090	9.597
1.639	6.950	0.318	0.603	12.410	0.274	13.510	0.692	1.113	14.463
0.366	14.300	0.358	0.545	15.514	0.400	9.410	0.538	1.157	10.809
0.297	14.830	0.360	0.537	15.813	*Garnet biotite gneiss (7)*				
0.459	12.820	0.365	0.599	14.348	0.313	9.170	0.228	0.526	10.207
0.315	16.430	0.387	0.523	17.473	0.358	9.150	0.232	0.529	10.334
0.294	16.540	0.393	0.529	17.515	0.369	7.690	0.200	0.531	8.912
0.350	16.590	0.427	0.567	17.751	0.274	9.670	0.239	0.533	10.579
Garnet biotite gneiss (5b)					0.358	8.210	0.213	0.534	9.395
0.610	15.140	0.367	0.505	17.156	0.318	9.940	0.249	0.535	10.994
0.437	16.300	0.386	0.514	17.746	0.299	9.580	0.240	0.536	10.570
0.429	12.690	0.313	0.524	14.110	0.315	9.800	0.247	0.537	10.845
0.640	16.380	0.412	0.525	18.499	0.417	11.020	0.285	0.542	12.401
0.433	12.230	0.306	0.528	13.665	0.302	9.610	0.244	0.543	10.612
0.640	14.880	0.381	0.529	16.999	0.395	9.810	0.256	0.544	11.120
0.477	12.560	0.318	0.531	14.140	0.311	9.100	0.235	0.546	10.133
0.649	7.210	0.213	0.537	9.360	0.366	9.300	0.244	0.548	10.515
1.152	18.610	0.512	0.539	22.429	0.362	10.600	0.275	0.550	11.802
0.650	9.900	0.276	0.540	12.053	0.345	10.320	0.268	0.551	11.464
1.348	16.370	0.478	0.541	20.839	0.301	9.560	0.247	0.552	10.559
0.654	15.780	0.415	0.545	17.947	0.338	9.470	0.248	0.553	10.593
0.945	16.580	0.456	0.546	19.713	0.316	9.680	0.252	0.554	10.729
0.673	18.500	0.481	0.547	20.732	0.320	9.550	0.250	0.555	10.613
0.738	12.070	0.338	0.548	14.518	0.342	10.140	0.266	0.557	11.274
0.459	8.590	0.235	0.549	10.111	0.513	7.960	0.229	0.558	9.662
1.266	15.860	0.468	0.551	20.061	0.372	10.720	0.283	0.559	11.957
0.435	7.500	0.209	0.552	8.943	0.556	7.220	0.216	0.561	9.068
0.710	10.510	0.302	0.553	12.866	0.337	9.410	0.251	0.562	10.531
0.762	16.070	0.437	0.554	18.598	0.303	9.550	0.252	0.562	10.557

Table A-8. *Contd.*

UO_2 (wt.%)	ThO_2 (wt.%)	PbO (wt.%)	Age (Ga)	ThO_2* (wt.%)
Garnet biotite gneiss (7) Contd.				
0.337	9.760	0.260	0.563	10.879
0.566	8.980	0.260	0.564	10.861
0.403	9.420	0.265	0.580	10.761
0.474	8.440	0.247	0.580	10.016
0.358	10.480	0.288	0.581	11.672
0.755	7.870	0.257	0.583	10.382
0.347	11.290	0.309	0.584	12.446
0.405	11.040	0.308	0.585	12.389
0.418	10.750	0.303	0.588	12.141
0.743	7.700	0.254	0.589	10.172
0.831	7.200	0.250	0.591	9.965
0.693	7.350	0.244	0.596	9.659
0.519	8.960	0.302	0.665	10.697
0.996	5.630	0.270	0.707	8.976
1.158	6.350	0.325	0.745	10.254
0.700	7.200	0.319	0.782	9.566
0.210	6.390	0.261	0.861	7.104
0.532	5.450	0.275	0.885	7.264
0.187	5.190	0.247	0.989	5.833
0.217	6.360	0.303	0.994	7.108
0.244	6.690	0.384	1.181	7.544
0.138	5.110	0.295	1.221	5.596
0.549	6.390	0.456	1.268	8.327
0.122	5.220	0.314	1.286	5.653
0.543	7.070	0.503	1.295	8.991
0.260	7.060	0.479	1.386	7.988
0.190	5.600	0.391	1.436	6.283
0.110	5.200	0.351	1.447	5.594
0.153	5.740	0.410	1.501	6.293
0.138	5.420	0.390	1.516	5.920
0.254	6.520	0.514	1.586	7.444
0.111	5.350	0.404	1.614	5.757
0.109	5.100	0.391	1.634	5.500
0.121	5.100	0.410	1.693	5.547
0.130	5.110	0.441	1.803	5.595
0.117	5.040	0.436	1.817	5.478
0.107	5.140	0.456	1.879	5.541
0.105	5.100	0.463	1.919	5.498
0.394	10.210	0.276	0.565	11.517
0.410	9.280	0.256	0.567	10.640
0.498	10.150	0.286	0.570	11.804
0.445	10.800	0.299	0.574	12.280
0.394	10.720	0.294	0.575	12.031
0.350	9.150	0.253	0.578	10.312

Table A-9. EPMA analyses of zircon and monazite from calc-silicate rock in the Nagercoil Block.

UO_2 (wt.%)	ThO_2 (wt.%)	PbO (wt.%)	Age (Ga)	ThO_2* (wt.%)
Zircon				
1.681	0.115	0.344	1.311	6.072
1.108	0.065	0.333	1.811	4.200

Table A-9. *Contd.*

UO_2 (wt.%)	ThO_2 (wt.%)	PbO (wt.%)	Age (Ga)	ThO_2* (wt.%)
Zircon Contd.				
1.078	0.081	0.293	1.664	4.040
0.482	0.137	0.252	2.637	2.137
0.634	0.042	0.178	1.711	2.381
0.440	0.023	0.117	1.645	1.636
0.223	0.015	0.063	1.720	0.838
0.207	0.012	0.056	1.661	0.771
0.181	0.010	0.041	1.442	0.660
0.151	0.013	0.041	1.649	0.566
0.135	0.012	0.040	1.770	0.513
0.072	0.018	0.029	2.214	0.298
0.286	0.029	0.028	0.670	0.986
0.094	0.000	0.028	1.793	0.351
0.255	0.023	0.025	0.674	0.877
0.273	0.040	0.023	0.581	0.947
0.230	0.029	0.022	0.658	0.799
0.265	0.033	0.022	0.573	0.915
0.203	0.012	0.022	0.737	0.697
0.252	0.037	0.021	0.573	0.876
0.270	0.036	0.021	0.540	0.929
0.266	0.037	0.021	0.542	0.920
0.263	0.031	0.021	0.549	0.904
0.177	0.019	0.020	0.780	0.616
Monazite				
0.255	7.120	0.183	0.541	7.966
0.248	6.430	0.170	0.551	7.253
0.270	6.630	0.166	0.521	7.523
0.251	6.430	0.164	0.534	7.262
0.260	5.930	0.145	0.505	6.790
0.262	5.680	0.144	0.518	6.547
0.257	5.670	0.143	0.519	6.521
0.260	5.430	0.138	0.518	6.291
0.265	5.010	0.128	0.513	5.886
0.254	4.020	0.107	0.521	4.860
0.225	3.630	0.094	0.508	4.374
0.223	3.590	0.099	0.540	4.328
0.267	11.670	0.298	0.560	12.557
0.252	11.790	0.296	0.554	12.627
0.637	9.250	0.269	0.558	11.365
0.930	6.740	0.233	0.558	9.828
0.909	6.700	0.228	0.554	9.716
0.905	6.640	0.240	0.585	9.650
0.925	6.640	0.236	0.573	9.714
0.900	6.610	0.233	0.572	9.602
0.896	6.590	0.232	0.572	9.566
0.902	6.570	0.232	0.573	9.567
1.048	6.380	0.239	0.572	9.863
1.024	6.330	0.236	0.572	9.732
0.972	7.580	0.274	0.598	10.816
0.178	6.040	0.527	1.796	6.704
0.214	8.300	0.662	1.670	9.087
0.330	6.580	0.342	1.032	7.719
1.203	7.310	0.292	0.608	11.320
0.476	8.580	0.243	0.563	10.160